

# Co-limitation of photosynthetic capacity by nitrogen and phosphorus in West Africa woodlands

TOMAS FERREIRA DOMINGUES<sup>1</sup>, PATRICK MEIR<sup>1</sup>, TED R. FELDPAUSCH<sup>2</sup>, GUSTAVO SAIZ<sup>3</sup>, ELMAR M. VEENENDAAL<sup>4</sup>, FRANZISKA SCHRODT<sup>3</sup>, MICHAEL BIRD<sup>2</sup>, GLORIA DJAGBLETEY<sup>5</sup>, FIDELE HIEN<sup>6</sup>, HALIDOU COMPAORE<sup>6</sup>, ADAMA DIALLO<sup>7</sup>, JOHN GRACE<sup>1</sup> & JON LLOYD<sup>2</sup>

<sup>1</sup>School of GeoSciences, University of Edinburgh, Drummond Street, Edinburgh, EH8 9XP, Scotland, UK, <sup>2</sup>Earth and Biosphere Institute, School of Geography, University of Leeds, LS2 9JT, Leeds, UK, <sup>3</sup>School of Geography & Geosciences, University of St Andrews, St Andrews, KY16 9AL, Scotland, UK, <sup>4</sup>Nature Conservation and Plant Ecology Group, Wageningen University, The Netherlands, <sup>5</sup>Forestry Research Institute of Ghana, Kumasi, Ghana, <sup>6</sup>Institut de l'Environnement et de Recherches Agricoles, Ouagadougou, Burkina Faso and <sup>7</sup>Centre National des Semences Forestières, Ouagadougou, Burkina Faso

## ABSTRACT

Photosynthetic leaf traits were determined for savanna and forest ecosystems in West Africa, spanning a large range in precipitation. Standardized major axis fits revealed important differences between our data and reported global relationships. Especially for sites in the drier areas, plants showed higher photosynthetic rates for a given N or P when compared with relationships from the global data set. The best multiple regression for the pooled data set estimated  $V_{\text{cmax}}$  and  $J_{\text{max}}$  from  $N_{\text{DW}}$  and  $S$ . However, the best regression for different vegetation types varied, suggesting that the scaling of photosynthesis with leaf traits changed with vegetation types. A new model is presented representing independent constraints by N and P on photosynthesis, which can be evaluated with or without interactions with  $S$ . It assumes that limitation of photosynthesis will result from the least abundant nutrient, thereby being less sensitive to the allocation of the non-limiting nutrient to non-photosynthetic pools. The model predicts an optimum proportionality for N and P, which is distinct for  $V_{\text{cmax}}$  and  $J_{\text{max}}$  and inversely proportional to  $S$ . Initial tests showed the model to predict  $V_{\text{cmax}}$  and  $J_{\text{max}}$  successfully for other tropical forests characterized by a range of different foliar N and P concentrations.

**Key-words:** A–C<sub>i</sub> curves; dry forest; NPP; savanna; tropical rain forest; photosynthesis.

## INTRODUCTION

The chemical composition of higher plant leaves and other foliar traits, such as leaf mass to area ratio ( $M_A$ ) and leaf longevity, generally co-vary with leaf photosynthetic rate,  $A$  (Reich, Walters & Ellsworth 1997; Wright *et al.* 2004). As photosynthesis is based on biochemical processes, scaling relationships are expected between photosynthetic capacity

and tissue chemical composition (e.g. Field & Mooney 1986; Evans 1989; Domingues *et al.* 2005). As understanding of these important relationships improves, relevant advances in leaf- and canopy-trait representations are gradually being incorporated into fine- and global-scale photosynthesis models (Sellers *et al.* 1997; Sitch *et al.* 2003; Ollinger & Smith 2005; Kattge *et al.* 2009; Xu, Gertner & Scheller 2009).

Despite the importance of globally representative data sets to global models, the bulk of previously published photosynthetic studies have been performed on model species or in temperate ecosystems, with some globally important areas remaining under-represented (Wright, Reich & Westoby 2001; Reich, Wright & Lusk 2007; Kattge *et al.* 2009). This bias in field data potentially undermines the accuracy of modelling efforts that use leaf traits as a basis for prediction of photosynthesis. A 'global spectrum' of positively and anticorrelated leaf traits has been discussed (Wright *et al.* 2004); however, substantial trait variability is evident within particular regions (e.g. Güsewell 2004; Reich & Oleksyn 2004; Wright *et al.* 2005a), making it difficult at present to justify a universal set of scaling relationships that functions equally well for all terrestrial ecosystems (Reich *et al.* 1999; Wright *et al.* 2006; Kattge *et al.* 2009). Probably the most important of these relationships is a recognized strong and positive correlation between photosynthetic capacity and leaf N (Field & Mooney 1986). Photosynthetic capacity is often described in plants by the maximum rate of carboxylation,  $V_{\text{cmax}}$ , which is in turn determined by the amount and activity of the enzyme ribulose 1,5-bisphosphate carboxylase/oxygenase (RuBisCO) (Farquhar, von Caemmerer & Berry 1980). Examination of the above-mentioned relationship has shown that photosynthetic capacity varies considerably with leaf nutrient content, especially N and P, with some of the biggest differences evident when temperate and tropical systems are compared (Reich & Schoettle 1988; Niinemets 1999; Kull 2002; Meir *et al.* 2002, 2007; Kattge *et al.* 2009). Temperate ecosystems are often considered to be limited by N (Schulze

Correspondence: T. F. Domingues. Fax: +44 (0) 131 650 2523; e-mail: tdomingu@staffmail.ed.ac.uk

*et al.* 1994). In contrast, several lines of evidence have suggested that many tropical forest soils have excess N (Högberg 1986; Martinelli *et al.* 1999; Okin *et al.* 2008), whereas the soils underlying many tropical forests and savannas are often highly weathered and are poor in total and plant available P (Vitousek & Sanford 1986; Lloyd *et al.* 2001; Hedin 2004; Reich & Oleksyn 2004; Lambers *et al.* 2008; Quesada *et al.* 2009a). Notwithstanding this general conclusion, however, examples to the contrary, of strong or partial N limitation in tropical forests exist for some savanna ecosystems (Lloyd *et al.* 2009), for forests growing on white sand soils such as Arenosols or Podzols (Martinelli *et al.* 1999; Mardegan *et al.* 2008), and for forests growing on the oldest and most infertile Ferralsol and Acrisol soil types in north-east and central Amazonia (Quesada *et al.* 2009b).

Temperate and boreal plants are thus expected to exhibit tight and steep  $V_{\text{cmax}}\text{-N}$  relationships, because N is generally limiting and its allocation to non-photosynthetic functions is expected to be minimized (Terashima *et al.* 2005). In contrast, in regions where N is relatively abundant but P availability is low, a weaker  $V_{\text{cmax}}\text{-N}$  relationship and a stronger  $V_{\text{cmax}}\text{-P}$  relationship might be anticipated. This has been observed, though not always as clearly as expected (Meir, Grace & Miranda 2001; Niinemets *et al.* 2001; Wright *et al.* 2004; Meir *et al.* 2007; Reich, Oleksyn & Wright 2009). Recently, Reich *et al.* (2009) presented evidence that high foliar P values are indeed related to a steeper slope of the relationship between saturating assimilation rate and leaf nitrogen content.

Several reasons have been proposed for the wide observed range in the proportion of woody versus herbaceous vegetation in tropical savannas, including the influence of rainfall, soil fertility, soil texture and moisture, and the local history of fire and grazing (e.g. Furley 1992; Lloyd *et al.* 2008). Although leaf-level properties do not necessarily explain differences in the distribution of vegetation types (Gifford & Evans 1981), two of these factors have provided the main focus for leaf gas exchange studies: fertility and rainfall, often with measurements taken over a transect spanning either or both environmental axes (e.g. Wright *et al.* 2001; Prior, Eamus & Bowman 2003; Midgley *et al.* 2004). There are, however, few leaf gas exchange measurements available for seasonally dry tropical biomes (Prado and de Moraes 1997; Franco 1998; Wright *et al.* 2001; Prior *et al.* 2003), especially for Africa (Mooney *et al.* 1983; Tuohy, Prior & Stewart 1991; Midgley *et al.* 2004; Meir *et al.* 2007). The few data that do exist show examples of lower area-based maximum photosynthetic rate at saturating irradiance ( $A_{\text{sat-A}}$ ) per unit N at drier sites (Wright *et al.* 2001; Midgley *et al.* 2004) and indicate that P is sometimes, but inconsistently, more strongly associated with  $A_{\text{sat-A}}$  than N (Tuohy *et al.* 1991; Wright *et al.* 2001, 2006; Prior *et al.* 2003; Meir *et al.* 2007).

Reliable estimates of the relationship between photosynthetic capacity and leaf nutrient content are particularly important for parameterizing terrestrial biosphere models (e.g. Woodward, Smith & Emanuel 1995; Niinemets 1999; Sitch *et al.* 2003; Reich *et al.* 2006; Raddatz *et al.* 2007).

Extending earlier work that examined the global co-ordination of leaf traits (Reich *et al.* 1997; Wright *et al.* 2004), Reich *et al.* (2007) highlighted the potential to estimate  $A_{\text{sat}}$  globally from phylogeny, plant growth form and leaf phenology, coupled with climatic data and easily measured leaf traits, such as  $M_A$  and N. Kattge *et al.* (2009) developed this approach for terrestrial biosphere models, focusing on the need to specify biochemical parameters such as  $V_{\text{cmax}}$  (Farquhar *et al.* 1980). A lower  $V_{\text{cmax}}$  per unit nitrogen has been reported for tropical forest leaves (Carswell *et al.* 2000; Domingues, Martinelli & Ehleringer 2007; Meir *et al.* 2007), and a potentially large negative impact of phosphorus-deficient tropical soils such as Ferralsols or Acrisols on the  $V_{\text{cmax}}\text{-N}$  relationship highlighted (Kattge *et al.* 2009). Although a lack of data hampers our understanding of how N and P constrain photosynthesis in tropical woody ecosystems, the data assimilation and modelling analysis approach of Kattge *et al.* (2009) yielded a much lower gross primary productivity for tropical forests compared with those obtained from earlier, more indirect, global estimates of photosynthetic parameters (e.g. Beerling & Quick 1995). This, in conjunction with the recent findings of Paoli & Curran (2007) and Quesada *et al.* (2009c) that soil phosphorus availability may be the key modulator of the above-ground net primary productivity of tropical forests in Borneo and Amazonia, respectively, underscores a strong need for more information on the role of phosphorus in modulating rates of carbon acquisition for tropical tree species, especially for ecosystems that experience seasonal water stress.

Here we present data on  $M_A$  (or specific leaf area,  $S = M_A^{-1}$ ,  $\text{m}^2 \text{g}^{-1}$ ), leaf N and P concentrations and leaf biochemical photosynthetic capacity ( $V_{\text{cmax}}$  and the electron transport capacity,  $J_{\text{max}}$ ) for woody vegetation along a 900 km north-south transect in West Africa, from Mali to Ghana, a globally important vegetation transition, yet one still poorly characterized. Although the biochemical transformations governed by  $V_{\text{cmax}}$  and  $J_{\text{max}}$  both require nitrogen and phosphorus, we expected  $V_{\text{cmax}}$  to be more strongly controlled by the amount of nitrogen present, because of the high N requirement by RuBisCO (Evans 1989). On the other hand we expected a stronger phosphorus constraint for  $J_{\text{max}}$  because of the many transformations of phosphorus-rich molecules (ATP, NADP and sugar-phosphates from the Calvin cycle) that occur for the regeneration of ribulose-1, 5-bisphosphate, RuBP (Farquhar *et al.* 1980; Woodrow & Berry 1988). Phosphorus is also an important component of phospholipid membranes, which might act as temporary storage for this element, changing membrane characteristics as phosphorus deficiency takes place (Tjellström *et al.* 2008). We examined vegetation types ranging from open savanna to different forms of woodland, and covering a large range in annual precipitation, with the (strong) dry season ( $<50 \text{ mm rainfall month}^{-1}$ ) ranging from 2 to 10 months (data from Climatic Research Unit, University of East Anglia, UK; New, Hulme & Jones 1999). We examined the following questions: (1) are data from this transect consistent with existing global leaf trait data sets?; (2) how strong are the  $V_{\text{cmax}}$  and  $J_{\text{max}}$

versus N relationships on both a dry-weight and an area basis?; (3) does P have a stronger influence over  $V_{\text{cmax}}$  and/or  $J_{\text{max}}$  than N?; (4) can we devise a general model to interpret and specify potential constraints on  $V_{\text{cmax}}$  and  $J_{\text{max}}$  by either N or P?

## MATERIALS AND METHODS

### Sites

Thirteen permanent 1 ha plots were established along a transect spanning 8.2 latitudinal degrees (900 km) over a precipitation range of 280–1450 mm  $\text{a}^{-1}$  in the west African countries of Mali, Burkina Faso and Ghana (Fig. 1a). Dry season length (number of months with precipitation <100 mm) ranged from 10 months in the north to 5 months in the south. The plots (Table 1) were located in different vegetation zones as described by White (1983): Hombori (arid end of Sudan savanna zone), Bissiga (moist end of Sudan savanna zone), Dano (Sudan savanna/Guinea savanna transition zone), Mole (Guinea savanna zone) and Kogyae, Boabeng-Fiema and Asukese (transitional zone between dry semi-deciduous forest and the Guinea savanna zone). The range of soils observed along the transect were classified according to the World Reference Base (WRB) (IUSS Working Group WRB 2006) as: Arenosols; Luvisols; Plinthosols; Alisols; Nitosols; and Fluvisols. Plot-specific allometric equations were developed relating stem diameter (1.3 m height, or above buttresses) to crown diameter. Distribution maps of trees for each plot were created in ArcMap (ESRI® ArcMap™ 9.1, Redlands, CA, USA) and used to overlay individual crowns and compute the plot level crown cover as the ratio of ground area that was covered by tree crowns.

Based on precipitation, vegetation physiognomy, tree crown cover and the categorizations of Keay (1949), Lloyd *et al.* (2008), and Lloyd *et al.* (2009), the plots fell into four natural groups, *viz* (1) open Sudan savanna (OSS), found at Hombori and Bissiga (precipitation <900 mm  $\text{a}^{-1}$ ); open savanna woodland (OSW), found at Dano and Mole (900 < precipitation < 1200 mm  $\text{a}^{-1}$ ); savanna woodland

(SW), found at Kogyae and Boabeng-Fiema plots 1 and 2 (precipitation > 1200 mm  $\text{a}^{-1}$ ), and dry semi-deciduous forest (SDF), found at Asukese and Boabeng-Fiema plots 3 and 4 (precipitation > 1200 mm  $\text{a}^{-1}$ ). See Table 1 for details.

### Gas exchange measurements

$\text{CO}_2$  response curves ( $A-C_i$  curves) were made on a total of 301 leaves taken from 39 species (105 individuals) of  $C_3$  woody plants, during the peak of the wet season of 2006, from August to September (Appendix A). The species sampled were chosen according to their quantitative representation in each permanent sample plot. Each plant was identified to species-level, either in the field, or where necessary, in the herbarium. All voucher specimens were returned to the herbarium at the Forestry Research Institute of Ghana (FORIG), at Kumasi for taxonomic verification. Two cross-calibrated Li-6400 portable photosynthesis systems (Li-Cor, Inc., Lincoln, NE, USA), each fitted with an artificial light source (6400-02B Red/Blue LED Light Source, Li-Cor, Inc.) were used to obtain the  $A-C_i$  curves following the procedural guidelines described in Long & Bernacchi (2003), with  $\text{CO}_2$  concentrations inside the chamber ranging from 50 to 2000 ppm. Only canopy-top leaves naturally exposed to direct sunlight (i.e. 'sun leaves') were used. Prior to the  $A-C_i$  measurements, tests were made to confirm that photosynthesis was light-saturated at a photosynthetically active radiation (PAR) flux density at or near 2000  $\mu\text{mol m}^{-2} \text{s}^{-1}$ . During the measurements, leaf temperature was controlled by conditioning the leaf chamber temperature to 30 °C (or exceptionally to 35 °C, depending on ambient temperature), with the vapour pressure deficit maintained at ambient levels.  $A_{\text{sat}}$ , obtained under saturating light and  $\text{CO}_2$  concentration inside the cuvette set to 400  $\mu\text{mol mol}^{-1}$ , was extracted from the  $A-C_i$  curves. Except when measuring the shrubby weed *Chromolaena odorata* (L.) R.M.King & H.Rob., to obtain access to leaves from tall tree species occurring in plots at Boabeng-Fiema, Asukese and Kogyae, large branches were detached and immediately re-cut under water in order to reconstitute xylem water continuity, and  $A-C_i$  curves were completed

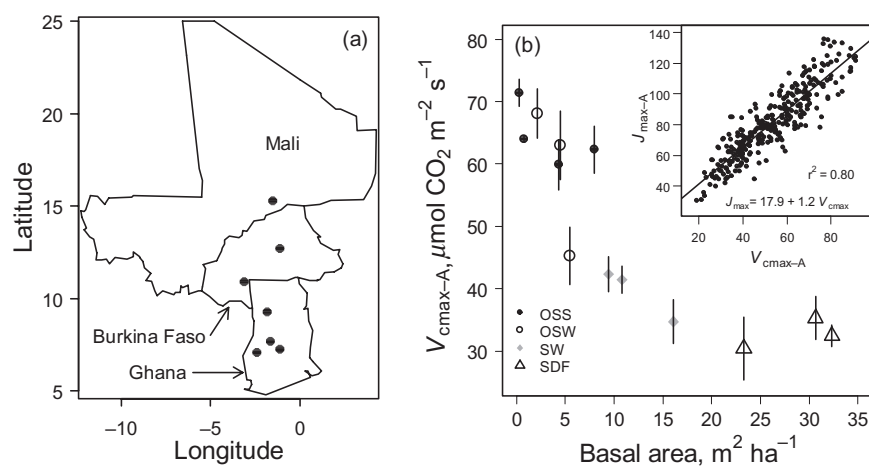


**Figure 1.** (a) Partial map of West Africa with location of the research sites. (b) The relationship between plot basal area (for trees with diameter >10 cm) and area based maximum carboxylation capacity ( $V_{\text{cmax-A}}$ ). Error bars are the standard error of the mean. Vegetation types: OSS, open Sudan savanna; OSW, open savanna woodland; SW, savanna woodland; SDF, semi-deciduous dry forest. The insert within Figure 1b shows the relationship between  $V_{\text{cmax-A}}$  and the area based electron transport capacity ( $J_{\text{max-A}}$ ).

**Table 1.** Characteristics of the plots sampled during the wet season of 2006; geographical coordinates; mean annual precipitation (MAP; mm a<sup>-1</sup>); soil classification; vegetation types; basal area of trees with diameter at breast height larger than 10 cm (m<sup>2</sup> ha<sup>-1</sup>); percent of tree ground area covered by tree crowns; and the leaf traits leaf mass to area ratio ( $M_A$ : g m<sup>-2</sup>), leaf nitrogen content ( $N_{DW}$ : g m<sup>-2</sup>), leaf phosphorus content ( $P_{DW}$ : g m<sup>-2</sup>), leaf-level light saturated carbon assimilation rates ( $A_{sat-A}$ ,  $\mu\text{mol m}^{-2} \text{s}^{-1}$ ), maximum carboxylation capacity ( $V_{cmax-A}$ :  $\mu\text{mol m}^{-2} \text{s}^{-1}$ ), and maximum rate of electron transport ( $J_{max-A}$ ,  $\mu\text{mol m}^{-2} \text{s}^{-1}$ ). Leaf trait values are averages among species sampled and standard deviation. Sample size indicates numbers of species sampled per plot, total individuals sampled per plot and total replicates per plot

Site	Lat. (N) Long. (W)	MAP	Soil type	Vegetation type	Basal area	Tree crown cover	Sample size: Species/ ind./total	$M_A$	$N_{DW}$	$P_{DW}$	$A_{sat-A}$	$V_{cmax-A}$	$J_{max-A}$
HOM-01	15.344 1.468	280	Rubic Arenosol (Dystric, Aridic)	Open Sudan savanna	0.28	1.1	2/4/10	111 ± 64	32.0 ± 21.1	1.84 ± 0.90	20.4 ± 1.7	71.4 ± 3.1	95.7 ± 5.6
HOM-02	15.335 1.547	280	Rubic Arenosol (Dystric, Aridic)	Open Sudan savanna	0.72	4.9	1/1/3	140	16.3	1.08	19.3	64.0	69.0
BBI-01	12.731 1.165	897	Haplic Luvisol (Epidystric, Endosiltic)	Open Sudan savanna	4.31	31.4	4/12/54	85 ± 31	23.0 ± 4.7	1.45 ± 0.16	15.7 ± 4.0	59.9 ± 8.1	85.3 ± 10.2
BBI-02	12.733 1.163	897	Pisolithic Plinthosol (Eutric)	Open Sudan savanna	8.02	50.9	3/9/26	106 ± 27	21.4 ± 6.1	1.08 ± 0.22	18.5 ± 1.1	62.4 ± 6.5	94.3 ± 8.2
BDA-01	10.940 3.149	1017	Acric Plinthosol (Mangani ferric, Dystric, Siltic)	Open savanna woodland	4.5	17.5	5/15/49	113 ± 29	14.6 ± 1.6	1.07 ± 0.18	18.4 ± 4.3	63.0 ± 12.3	92.7 ± 13
BDA-02	10.940 3.154	1017	Pisolithic Plinthosol (Mangani ferric, Dystric, Siltic)	Open savanna woodland	2.12	2.62	3/9/28	150 ± 45	13.4 ± 0.9	0.92 ± 0.05	20.7 ± 0.4	68.1 ± 6.8	104.6 ± 17.2
MLE-01	9.304 1.858	1188	Brunic Arenosol (Dystric)	Open savanna woodland	5.48	25.7	4/12/37	122 ± 15	13.5 ± 1.2	0.96 ± 0.16	12.9 ± 3.9	45.2 ± 10.2	74.1 ± 13.9
KOG-01	7.302 1.180	1453	Haplic Arenosol (Dystric)	Savanna woodland	10.8	44.1	8/11/19	97 ± 31	19 ± 4.8	1.69 ± 0.52	10.1 ± 2.6	41.4 ± 6.2	67.6 ± 10.4
BFI-01	7.714 1.694	1302	Haplic Alisol (Arenic, Hyperdystric, Rhodic)	Savanna woodland	16.1	45.6	3/4/13	62 ± 5	24.6 ± 3	2.12 ± 0.39	6.8 ± 1.1	34.7 ± 6.1	72.0 ± 9.3
BFI-02	7.715 1.692	1302	Brunic Arenosol (Alumic, Hyperdystric)	Savanna woodland	9.45	59.2	6/7/16	119 ± 25	17.1 ± 1.2	1.23 ± 0.29	10.6 ± 1.8	42.3 ± 6.8	67.2 ± 14.3
BFI-03	7.705 1.696	1302	Haplic Nitosol (Dystric)	Semi-deciduous dry forest	30.7	66.4	5/7/16	83 ± 18	23.4 ± 4.5	1.29 ± 0.38	9.0 ± 2.8	35.3 ± 7.7	61.2 ± 7.8
BFI-04	7.708 1.698	1302	Haplic Nitosol (Dystric)	Semi-deciduous dry forest	32.3	80.8	6/6/11	76 ± 20	24.4 ± 4.6	1.59 ± 0.49	8.1 ± 1.8	32.4 ± 4.3	50.4 ± 7.3
ASU-01	7.137 2.447	1271	Endofluvic Cambisol (Dystric)	Semi-deciduous dry forest	23.3	65.1	4/5/10	64 ± 10	29.6 ± 3.8	1.37 ± 0.38	7.7 ± 2.5	30.4 ± 10.1	50.4 ± 17.9

ASU, Asukesc, Ghana; BBI, Bissiga Burkina-Faso; BFI, Boabeng-Fiema, Ghana; BDA, Dano, Burkina-Faso; HOM, Hombori, Mali; MLE, Mole, Ghana; KOG, Kogyae, Ghana.

within about 30 min. Alterations in stomatal conductance ( $g_s$ ) resulting from this process do not affect the calculation of  $V_{\text{cmax}}$  unless  $g_s$  declines to very low levels (Santiago & Mulkey 2003); in these instances (20% of cases, 16 out of 82) data were discarded from the analysis. A further check on data quality used elsewhere (Kattge *et al.* 2009) was also applied: where  $A_{\text{sat}}/N_{\text{DW}} < 2 \mu\text{mol CO}_2 \text{ g N}^{-1} \text{ s}^{-1}$ , data were also excluded (<1% of leaves).

### Response curve analyses

A curve fitting routine based on minimum least-squares (Appendix B) was developed for use with the 'R' environment (R Development Core Team 2008) to calculate  $V_{\text{cmax}}$ ,  $J_{\text{max}}$ , the rate of phosphate release resulting from triose phosphate utilization (TPU) and the daytime rate of mitochondrial respiration ( $R_d$ ). The fits were obtained using the Farquhar biochemical model of leaf photosynthesis (Farquhar *et al.* 1980; von Caemmerer 2000), with a modification for TPU by Harley *et al.* (1992). The enzymatic kinetic constants were taken from von Caemmerer (2000), assuming an infinite internal conductance term. For comparison with existing data on  $V_{\text{cmax}}$  (e.g. Wullschlegel 1993; Kattge *et al.* 2009), the fitted parameters ( $V_{\text{cmax}}$  and  $J_{\text{max}}$ ) presented here were scaled to a reference temperature of 25 °C using updated temperature dependencies provided by Bernacchi, Pimentel & Long (2003). A curve-fitting strategy was chosen to avoid the co-limited region of the  $A-C_i$  response curve:  $V_{\text{cmax}}$  was only fitted to values of intercellular  $\text{CO}_2$  concentrations ( $C_i$ ) lower than 30 Pa, whereas  $J_{\text{max}}$  was only fitted to  $C_i$  values higher than 45 Pa. The TPU function was fitted to the highest  $C_i$  values in each response curve.

### Nutrient analyses

Immediately following gas exchange determinations, individual leaves were detached and stored in a re-sealable plastic bag containing a piece of paper tissue and a few millilitres of water in order to allow full leaf hydration (Prior *et al.* 2003). After a minimum of 5 h and a maximum of 34 h, leaves were scanned with a flat-bed digital scanner and transferred to paper envelopes. The leaves were then dried to constant mass at 60 °C in convection ovens and their dry mass recorded to obtain  $M_A$ . Leaf area was determined from scanned images using Winfolia<sup>tm</sup> software (2005, Regent Instruments Inc., Ottawa, Canada). Mass-based leaf carbon content ( $C_{\text{DW}}$ ) and mass-based leaf nitrogen content ( $N_{\text{DW}}$ ) were determined by elemental analysis (EURO EA CHNSO Analyser, HEKAtech GmbH, Wegberg, Germany), with mass-based leaf phosphorus content ( $P_{\text{DW}}$ ) determined by inductively coupled plasma optical emissions spectrometry (ICP-OES) (PerkinElmer Optima 5300DV, PerkinElmer, Shelton, CT, USA) after nitric-perchloric digestion.

### Statistical analyses

A full survey of all species was not practical at each site, so quantitatively important (and physically measurable)

species were used. As a consequence, true species-weighted plot-level estimates of mean photosynthetic capacity were not achievable. However, to obtain coarse plot-level comparisons of mean parameter values, leaf replicates from individual trees were averaged and then the average of all individuals was taken for each species sampled at each site to enable a final cross-species average (number of species per site = 2–8, except Hom-2, see Table 1). To test for differences among plots, non-parametric Wilcoxon/Kruskal-Wallis tests (rank sums) were applied using a significance threshold of  $P < 0.05$  (JMP software version 5.0.1.2, SAS Institute, Cary, NC, USA).

Subsequent analysis of leaf gas exchange parameters, leaf nutrient and leaf structure data was made on an individual leaf basis and on  $\log_{10}$  transformed data. Although the fundamental biochemical photosynthetic parameters  $V_{\text{cmax}}$  and  $J_{\text{max}}$  were derived for each leaf, the composite gas exchange measure of  $A_{\text{sat}}$  was also examined in bivariate relationships with  $M_A$ , N and P to compare with existing global data sets (Reich *et al.* 1997; Wright *et al.* 2004), using standardized major axis (SMA) regression fits (Warton *et al.* 2006; Wright *et al.* 2006). Exploratory regression analysis was then performed on  $V_{\text{cmax}}$  and  $J_{\text{max}}$  with respect to  $M_A$ , N and P, with the relationships between nutrient content and the two photosynthetic capacity parameters being analysed on both a dry-weight and leaf area basis. Data were analysed either as a composite group (all sites combined), or by individual vegetation type (Table 2). This was followed by a comparison of SMA slopes from vegetation types for which statistically significant standard regressions had already been obtained (Fig. 2). Stepwise multiple linear regression analysis was also used to quantify the relationships between  $V_{\text{cmax}}$  and  $J_{\text{max}}$  and multiple leaf traits (N, P and  $M_A$ ), which are presented in Table 2. As was also observed by Reich *et al.* (2007), the interaction terms for these regressions were mostly non-significant and, when significant, their inclusion did not explain much additional variation in the dependent variable. Such interaction terms have thus been excluded from the analyses reported here. An analysis of partial correlations between mass-based photosynthetic capacity parameters and  $N_{\text{DW}}$ ,  $P_{\text{DW}}$ , and  $S$  was performed to examine the relative importance of each leaf trait for the different vegetation formations (Table 3).

Finally, we examined two variations of a new model framework that considers the different and independent roles of N and P in constraining both  $V_{\text{cmax}}$  and  $J_{\text{max}}$ . First, the relationship between leaf nutrient content and photosynthetic capacity was modelled as:

$$\begin{aligned} V_{\text{cmax}} &= \min \{ \alpha_N + v_N N, \alpha_P + v_P P \} \\ J_{\text{max}} &= \min \{ \gamma_N + \varepsilon_N N, \gamma_P + \varepsilon_P P \} \end{aligned} \quad (1)$$

where  $\alpha_N$ ,  $v_N$ ,  $\alpha_P$ ,  $v_P$ ,  $\gamma_N$ ,  $\varepsilon_N$ ,  $\gamma_P$  and  $\varepsilon_P$  are all empirical coefficients. This model assumes that the least available nutrient independently constrains the maximum value for  $V_{\text{cmax}}$  or  $J_{\text{max}}$ . The fitting procedure allows for the possibility that, although both N and P can simultaneously influence  $V_{\text{cmax}}$  and  $J_{\text{max}}$ , these two photosynthetic parameters may scale

Model	All data	OSS	OSW	SW	SDF
$V_{\text{cmax-DW}} = a + b * N_{\text{DW}}$	0.29	0.58	0.36	0.42	0.20
$V_{\text{cmax-DW}} = a + b * P_{\text{DW}}$	0.20	0.37	0.17	0.44	0.25
$V_{\text{cmax-DW}} = a + b * S$	0.32	0.66	0.23	0.58	0.47
$V_{\text{cmax-DW}} = a + b * N_{\text{DW}} + c * P_{\text{DW}}$	0.31	0.62	0.41	0.60	ns
$V_{\text{cmax-DW}} = a + b * N_{\text{DW}} + c * S$	0.36	0.79	0.42	ns	ns
$V_{\text{cmax-DW}} = a + b * P_{\text{DW}} + c * S$	0.33	0.68	0.32	0.62	ns
$V_{\text{cmax-DW}} = a + b * N_{\text{DW}} + c * P_{\text{DW}} + d * S$	ns	ns	0.46	ns	ns
$J_{\text{max-DW}} = c + d * N_{\text{DW}}$	0.35	0.52	0.42	0.49	0.22
$J_{\text{max-DW}} = c + d * P_{\text{DW}}$	0.26	0.30	0.15	0.48	0.20
$J_{\text{max-DW}} = c + d * S$	0.43	0.67	0.26	0.63	0.37
$J_{\text{max-DW}} = d + e * N_{\text{DW}} + f * P_{\text{DW}}$	0.38	0.54	0.45	0.67	ns
$J_{\text{max-DW}} = d + e * N_{\text{DW}} + f * S$	0.47	0.77	0.49	ns	ns
$J_{\text{max-DW}} = d + e * P_{\text{DW}} + f * S$	0.45	ns	0.32	0.68	0.40
$J_{\text{max-DW}} = e + f * N_{\text{DW}} + g * P_{\text{DW}} + h * S$	ns	ns	0.50	0.71	ns

Coefficients are not shown when  $P > 0.05$ . ns, non-significant; OSS, open Sudan savanna; OSW, open savanna woodland; SW, savanna woodland; DF, semi-deciduous dry forest.

**Table 2.** Coefficients of determination of linear regressions produced between leaf photosynthetic capacity and leaf traits ( $V_{\text{max-DW}}$  and  $J_{\text{max-DW}}$ ) and leaf traits (nitrogen content,  $N_{\text{DW}}$ ; phosphorus content,  $P_{\text{DW}}$ ; and specific leaf area,  $S$ ), for  $\log_{10}$  transformed data

differentially with each nutrient, each relationship requiring a separate slope and intercept term (cf. Field & Mooney 1986; Takashima, Hikosaka & Hirose 2004; Harrison *et al.* 2009). For example, *a priori*, we might expect  $V_{\text{cmax}}$  to track the availability of nitrogen more closely than that of phosphorus because of the nitrogen demand from RuBisCO,

whereas  $J_{\text{max}}$  may be correlated more closely with phosphorus content because of the importance of that element in mediating the regeneration of RuBP (see Introduction). Consequently, this framework allows for one nutrient to be in excess in relation to the other, presumably being part of a non-photosynthetic pool.

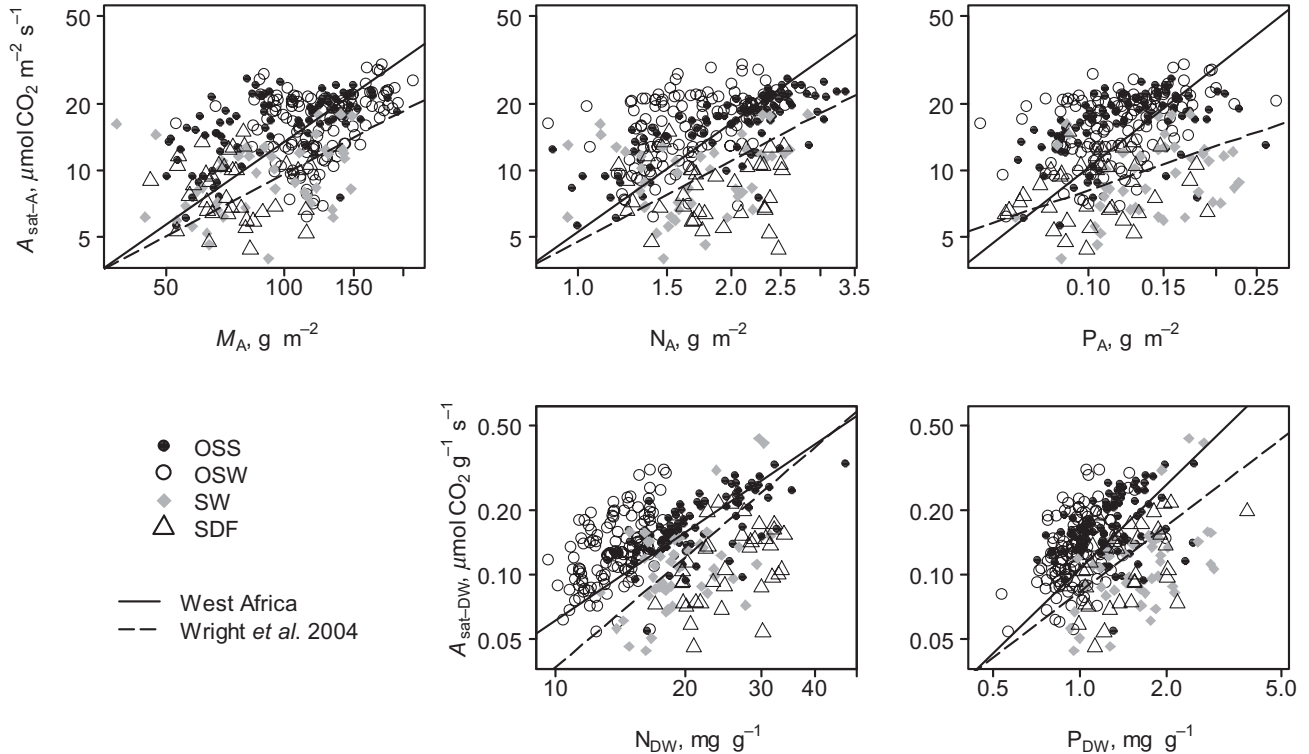


**Figure 2.** The relationships between leaf structure represented as leaf mass to area ratio ( $M_A$ ), leaf nutrient content (nitrogen and phosphorus), and leaf-level light saturated assimilation rates ( $A_{\text{sat}}$ ). Axes are in  $\log_{10}$  scale. Full lines refer to standardized major axis Standardized major axis (SMA) line-fitting applied to the whole data set. Dashed lines are SMA fits from a global data set presented by Wright *et al.* (2004). The slopes of the lines are significantly different between each other in each graph ( $P < 0.05$ ). The individual sites names are given with vegetation type as per Figure 1 in parentheses.

**Table 3.** Summary of partial correlations among leaf photosynthetic capacity ( $V_{\text{cmax-DW}}$  and  $J_{\text{max-DW}}$ ) and leaf traits (nitrogen content,  $N_{\text{DW}}$ ; phosphorus content,  $P_{\text{DW}}$  and the specific leaf area,  $S$ ), based on  $\log_{10}$  transformed data

	All data	OSS	OSW	SW	SDF
$V_{\text{cmax-DW}}$					
$N_{\text{DW}}$	0.219	0.584	0.453	0.242	0.196
$P_{\text{DW}}$	0.058	0.058	0.245	0.345	0.196
$S$	0.286	0.671	0.286	0.333	0.536
$J_{\text{max-DW}}$					
$N_{\text{DW}}$	0.224	0.543	0.516	0.323	0.265
$P_{\text{DW}}$	0.074	-0.098	0.187	0.392	0.147
$S$	0.392	0.705	0.320	0.353	0.444

Significant correlations were observed for all paired comparisons ( $P < 0.05$ ).

OSS, open Sudan savanna; OSW, open savanna woodland; SW, savanna woodland; SDF, semi-deciduous dry forest.

Eqn 1 estimates the combined influence of N and P on  $V_{\text{cmax}}$  and  $J_{\text{max}}$  (with values expressed on either a dry weight or area basis) and was fitted using an iterative minimum least-squares procedure, based on the BFGS optimization method (Nocedal & Wright 2006) embedded in 'R' (R Development Core Team, 2008 – package 'stats', version 2.8.0, function 'optim').

We also evaluated a variation of Eqn 1 where leaf structure is taken into account, allowing for N and P to scale independently with  $S$ :

$$\begin{aligned} V_{\text{cmax}} &= \min \{ \alpha_N + v_N N + \sigma_N S, \alpha_P + v_P P + \sigma_P S \} \\ J_{\text{max}} &= \min \{ \gamma_N + \varepsilon_N N + \zeta_N S, \gamma_P + \varepsilon_P P + \zeta_P S \} \end{aligned} \quad (2)$$

where  $\alpha_N$ ,  $v_N$ ,  $\sigma_N$ ,  $\alpha_P$ ,  $v_P$ ,  $\sigma_P$ ,  $\gamma_N$ ,  $\varepsilon_N$ ,  $\zeta_N$ ,  $\gamma_P$ ,  $\varepsilon_P$ , and  $\zeta_P$  are all empirical coefficients. This variation of the model accommodates the fact that thick leaves might have more N allocated to non-photosynthetic pools such as cell walls.

The Akaike Information Criterion (AIC; Akaike 1974) was used to compare standard models (multiple regressions) with the results from the fits to Eqns 1 and 2 (Table 4).

## RESULTS

### Variability among plots

Average area-based  $V_{\text{cmax}}$  ranged from 19 to 91  $\mu\text{mol m}^{-2} \text{s}^{-1}$  with average species values for  $J_{\text{max}}$  varying from 31 to 136  $\mu\text{mol m}^{-2} \text{s}^{-1}$ . The regression of  $J_{\text{max-A}}$  on  $V_{\text{cmax-A}}$  suggested tight co-ordination between the two photosynthetic parameters ( $P < 0.001$ ,  $r^2 = 0.80$ ,  $n = 301$ ) with a slope of  $1.2 \pm 0.03$  (standard error) (Fig. 1b, inset). The association between plot basal area and mean  $V_{\text{cmax-A}}$  was negative and curvilinear with the highest photosynthetic capacities observed for trees in the OSS and OSW vegetation types (Fig. 1b). Significant differences among plots were found for  $N_{\text{DW}}$  and  $P_{\text{DW}}$  but no statistical distinction among plots was found when area-based leaf nitrogen ( $N_A$ ) or leaf phosphorus ( $P_A$ ) was considered. Significant differences were

observed among plots for  $M_A$ , with larger values associated with a smaller basal area and lower annual precipitation at each plot. All photosynthetic capacity parameters obtained from the  $A-C_i$  curves ( $A_{\text{sat}}$ ,  $V_{\text{cmax}}$  and  $J_{\text{max}}$ ; Table 1) showed significant differences among plots on both mass and area bases, except for mass-based  $R_d$  (data not shown), for which differences were marginally non-significant ( $P = 0.06$ ).

### Maximum assimilation rate

Bivariate linear regressions of  $A_{\text{sat}}$  on  $M_A$ , N and P (either area or mass basis for nutrients) were highly significant ( $P < 0.001$ ) when all data were pooled. When the data were grouped by vegetation type a similar result was obtained, although significant area-based relationships were not obtained for SW or SDF (data not shown). The slopes of the SMA fits for the pooled bivariate relationships (Fig. 2) were significantly different ( $P < 0.05$ ) from the SMA fits to  $A_{\text{sat}}$  presented for a global data set by Wright *et al.* (2004).

### Photosynthetic capacity

Using the pooled data set and data separated by vegetation type, significant bivariate regressions were obtained for  $V_{\text{cmax}}$  and  $J_{\text{max}}$  on  $M_A$ , N and P (with leaf nutrients expressed on both mass- and area-bases; Table 2 and Appendix C, respectively). The explanatory power of individual leaf traits as determined by the regression coefficient ( $r^2$ ) varied from 0.12 to 0.47 (Table 2 and Appendix C), with substantially better relationships when the variables were expressed on a mass basis. SMA analyses made on an area basis (Fig. 3) identified both differences and similarities among vegetation types. For example, the slope of  $V_{\text{cmax-A}}$  on  $N_A$  was not different between OSW and either OSS or SW, but was distinct ( $P < 0.05$ ) for the other vegetation type comparisons. The SMA slopes of  $V_{\text{cmax-A}}$  on  $P_A$  were not different for SW versus OSS trees but were significantly different ( $P < 0.05$ ) between OSS and OSW. Finally, the SMA slopes of  $V_{\text{cmax-A}}$  on  $M_A$ , were significantly different ( $P < 0.05$ ) for almost all vegetation type contrasts, except between OSW and SW. An identical pattern was obtained when these analyses were repeated for  $J_{\text{max}}$  expressed on an area basis. Our results thus suggest that nutrient limitation of photosynthesis may have changed with vegetation type along the transect.

### Estimating photosynthetic capacity from multiple leaf traits

Multiple regression analysis explained more variation in the data ( $r^2 = 0.31-0.79$ , Table 2) than the bivariate comparisons. The best regressions were obtained using mass-based expressions of each variable. As  $V_{\text{cmax}}$  and  $J_{\text{max}}$  can be easily transformed from mass-based to area-based values for modelling purposes via  $M_A$  (which tends to be widely available for different vegetation types), we report mass-based multiple regression results in Table 2, and give the area-based analysis results in Appendix C. The model that

Model	Mass basis and log <sub>10</sub>		Area basis and log <sub>10</sub>	
	<i>r</i> <sup>2</sup>	AIC	<i>r</i> <sup>2</sup>	AIC
$V_{\text{cmax-DW}} = a + bN_{\text{DW}} + cP_{\text{DW}}$	0.31	-370.6	0.22	-376.6
$V_{\text{cmax-DW}} = \min\{\alpha_N + v_N N_{\text{DW}}; \alpha_P + v_P P_{\text{DW}}\}$	<b>0.32</b>	<b>-376.7</b>	0.25	-390.8
$J_{\text{max-DW}} = a + bN_{\text{DW}} + cP_{\text{DW}}$	0.38	-436.0	0.22	-468.3
$J_{\text{max-DW}} = \min\{\gamma_N + \varepsilon_N N_{\text{DW}}; \gamma_P + \varepsilon_P P_{\text{DW}}\}$	<b>0.40</b>	<b>-441.9</b>	0.27	-484.3

Model selection follow a combination of higher *r*<sup>2</sup> (same row) and smaller values of AIC's (same column) for each parameter ( $V_{\text{cmax}}$  or  $J_{\text{max}}$ ), which are presented in bold.

explained the most variation in  $V_{\text{cmax-DW}}$  and  $J_{\text{max-DW}}$  for the pooled data set was a multiple regression based on  $N_{\text{DW}}$  and  $S$ , *r*<sup>2</sup> = 0.36 and 0.47 for  $V_{\text{cmax-DW}}$  and  $J_{\text{max-DW}}$ , respectively ( $P < 0.05$ ) although the spread of the residuals was uneven among vegetation types (Fig. 4a, b, Table 2). Selection of the best vegetation-specific regressions yielded more homoscedastic residuals (Fig. 4c, d, Table 2) with the regression of  $V_{\text{cmax-DW}}$  on  $N_{\text{DW}}$  and  $S$  explaining the greatest variation for OSS trees (*r*<sup>2</sup> = 0.79,  $P < 0.05$ ), but with the regression of  $V_{\text{cmax-DW}}$  on  $P_{\text{DW}}$  and  $S$  being the best combination for SW trees (*r*<sup>2</sup> = 0.62,  $P < 0.05$ ). For OSW,  $V_{\text{cmax-DW}}$  was best described using a three-factor model based on  $N_{\text{DW}}$ ,  $P_{\text{DW}}$  and  $S$  (*r*<sup>2</sup> = 0.46,  $P < 0.05$ ) whereas for the SDF sites, the regression of  $V_{\text{cmax-DW}}$  on  $S$  (*r*<sup>2</sup> = 0.47,  $P < 0.05$ ) could not be improved upon by inclusion of leaf nutrient data, although for  $J_{\text{max-DW}}$  the best relationship combined  $P_{\text{DW}}$  and  $S$  (*r*<sup>2</sup> = 0.40,  $P < 0.05$ ). For the other vegetation types the regression results for  $J_{\text{max-DW}}$  were similar to those for  $V_{\text{cmax-DW}}$  (Table 2). When these analyses were repeated using area-based trait measures, similar patterns were found with two exceptions: for SDF, no significant regressions were obtained for  $V_{\text{cmax-A}}$  with any area-based trait; and, for SW, the best regression did not include  $M_A$  or  $N_A$ , but a significant role was found for  $P_A$  (*r*<sup>2</sup> = 0.18,  $P < 0.05$ ,

Appendix C). These outcomes were underlined in the partial correlation results, which identified phosphorus as constraining  $V_{\text{cmax-DW}}$  most strongly for trees growing at the SW sites (Table 3).

The possibility of either N or P limiting photosynthetic capacity was further probed by fitting Eqn 1 to all  $V_{\text{cmax}}$  and  $J_{\text{max}}$  values (log<sub>10</sub>-transformed data, as elsewhere), to examine overall nutrient constraints on  $V_{\text{cmax}}$  and  $J_{\text{max}}$  across the study transect. Mass-based analyses produced models with larger *r*<sup>2</sup> when compared with their area-based counterparts (Table 4). Equation 1 returned the lowest AIC values when compared with the corresponding multiple regression models, suggesting 'better' model performance as determined by goodness of fit and parsimony with respect to the number of fitted parameters (Burnham and Anderson 2002). The outputs for the best fit model using Eqn 1 for  $V_{\text{cmax-DW}}$  and  $J_{\text{max-DW}}$  are shown in Fig. 5a, b; the proportion of data points that are phosphorus-constrained for  $V_{\text{cmax-DW}}$  was 0.33, and for  $J_{\text{max-DW}}$  was 0.45 (blue points in Fig. 5). Further examination of the model output suggested a slight tendency for overestimation of photosynthetic capacity at high values and underestimation at low  $V_{\text{cmax-DW}}$  and  $J_{\text{max-DW}}$  (Fig. 5c,d). When Eqn 1 was fitted directly to area-based leaf trait values, similar model fits were

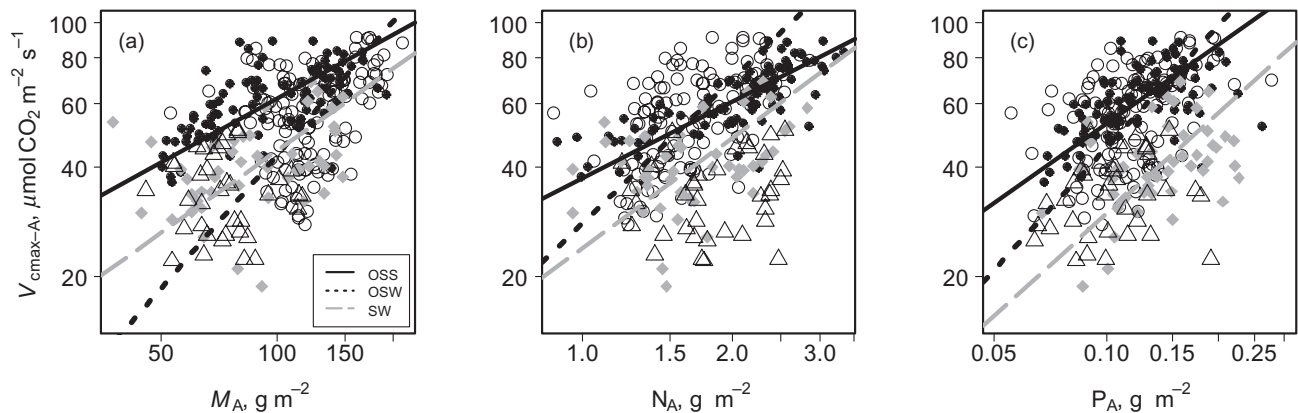


**Figure 3.** Standardized major axis (SMA) fits between log<sub>10</sub> transformed photosynthetic capacity ( $V_{\text{cmax}}$ ) and leaf traits. Axes are in log<sub>10</sub> scale. Vegetation type is denoted as per Figure 1; data from semi-deciduous dry forest (SDF) were not plotted as the relevant bivariate linear regressions were not significant. (a) the SMA slopes were significantly different between open Sudan savanna (OSS) and open savanna woodland (OSW), and between OSW and SW, but similar between OSS and savanna woodland (SW); (b) the SMA slope for OSS was significantly different from the slopes for OSW and SW, but there were no differences between the slopes for OSW and SW; (c) the SMA slopes were significantly different between OSS and OSW, but similar for OSS and SW and OSW and SW ( $\alpha = 0.05$ ). Symbols follow Figure 1 legend.

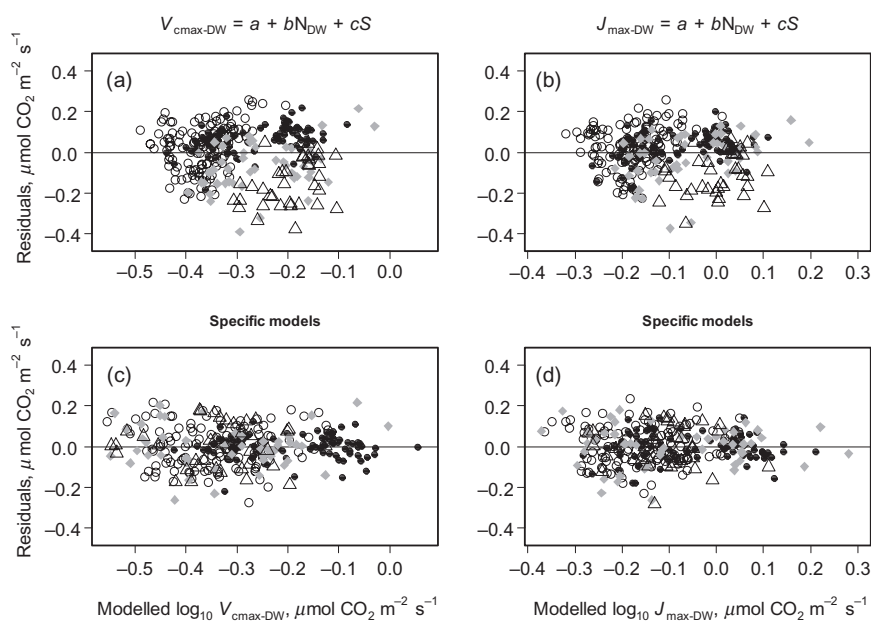


**Figure 4.** Residuals from regression models used to estimate  $V_{cmax-DW}$  and  $J_{max-DW}$  ( $\log_{10}$ ) based on mass based leaf nutrients and/or structure (Table 2). (a) and (b) represent the model that best described the whole data set. (c) and (d) are a composite of the specific models that fitted best to each separate vegetation type (Table 2). The specific models are: OSS:  $\log_{10} V_{cmax-DW} = a + b \log_{10} N_{DW} + c \log_{10} S$ ; OSW:  $\log_{10} V_{cmax-DW} = a + b \log_{10} N_{DW} + c \log_{10} P_{DW} + d \log_{10} S$ ; SW:  $\log_{10} V_{cmax-DW} = a + b \log_{10} P_{DW} + c \log_{10} S$ ,  $\log_{10} J_{max-DW} = a + b \log_{10} N_{DW} + c \log_{10} P_{DW} + d \log_{10} S$ ; and SDF:  $\log_{10} V_{cmax-DW} = a + b \log_{10} S$ ,  $\log_{10} J_{max-DW} = a + b \log_{10} P_{DW} + c \log_{10} S$ . Symbols and vegetation abbreviations follow Figure 1.

obtained, although the relationships were somewhat weaker (Table 4).

As the inclusion of a third parameter could potentially affect model performance, the influence on model outcome of other leaf nutrients as well as leaf structure was evaluated. Foliar concentrations of Mg, K, Ca, S, Mn, and Al failed to produce a third significant parameter for Eqn 1. However, the influence exerted by  $S$  over photosynthetic capacity (Table 2 and Appendix C) was visible in an improved

distribution of model residuals (Fig. 6). Overall, within each vegetation type, the slopes of linear regressions between  $S$  and the model residuals were significantly positive, stressing the relevance of that variable on model predictions.

The capacity of the new framework to predict photosynthetic capacity was thus substantially improved with the incorporation of  $S$  as a parameter (Fig. 7). For a given combination of leaf N and P, photosynthetic capacity increased with decreasing  $S$ . Disregarding possible variations in leaf

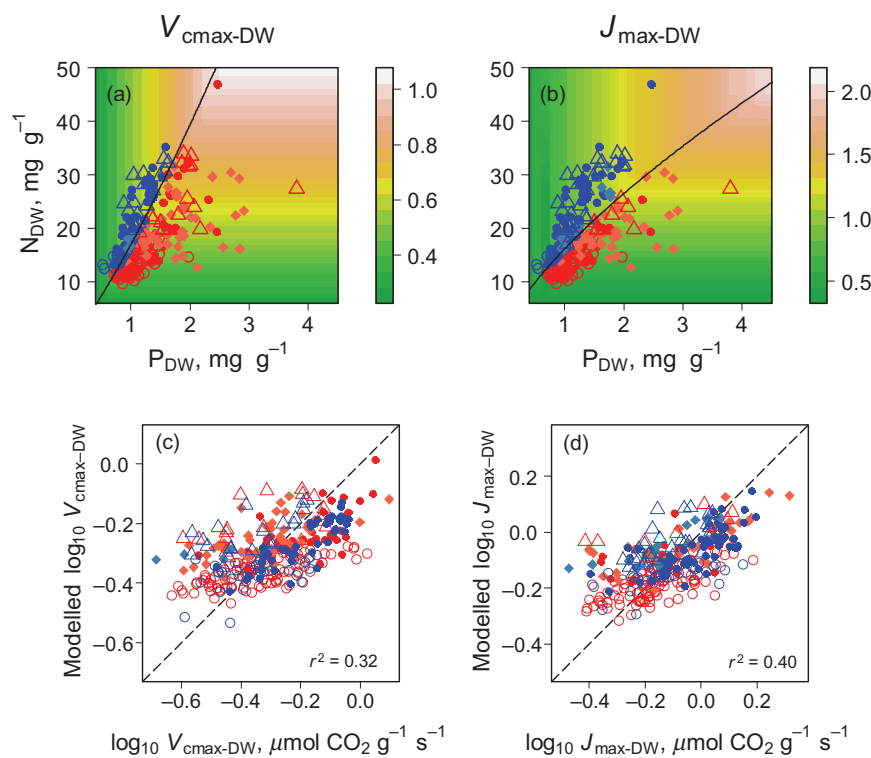


**Figure 5.** The combined constraint on photosynthetic capacity from nitrogen and phosphorus according to Eqn 1: (a)  $\log_{10} V_{cmax-DW} = \min[(\alpha_N + v_N * \log_{10} N_{DW}); (\alpha_P + v_P * \log_{10} P_{DW})]$ , where  $\alpha_N = -1.16$ ;  $v_N = 0.70$ ;  $\alpha_P = -0.30$ ; and  $v_P = 0.85$  and (b)  $\log_{10} J_{max-DW} = \min[(\gamma_N + \epsilon_N * \log_{10} N_{DW}); (\gamma_P + \epsilon_P * \log_{10} P_{DW})]$ , where  $\gamma_N = -1.22$ ;  $\epsilon_N = 0.92$ ;  $\gamma_P = -0.11$ ; and  $\epsilon_P = 0.66$ . The model outputs were subsequently reconverted to normal scale and are represented by the coloured scale through interpolation of  $N_{DW}$ ,  $P_{DW}$  and model outputs. Blue symbols represent the fraction of the data set where  $P_{DW}$  was the limiting nutrient and red symbols correspond to limitation by  $N_{DW}$ . The line on graph (a) is described as  $P_{DW} = 0.097 * (N_{DW})^{0.82}$  and on graph (b) as  $P_{DW} = 0.021 * (N_{DW})^{1.4}$ . Symbols and vegetation abbreviations follow Figure 1. Model performance for  $V_{cmax}$  and  $J_{max}$  is presented as observations against predictions on (c) and (d), respectively.

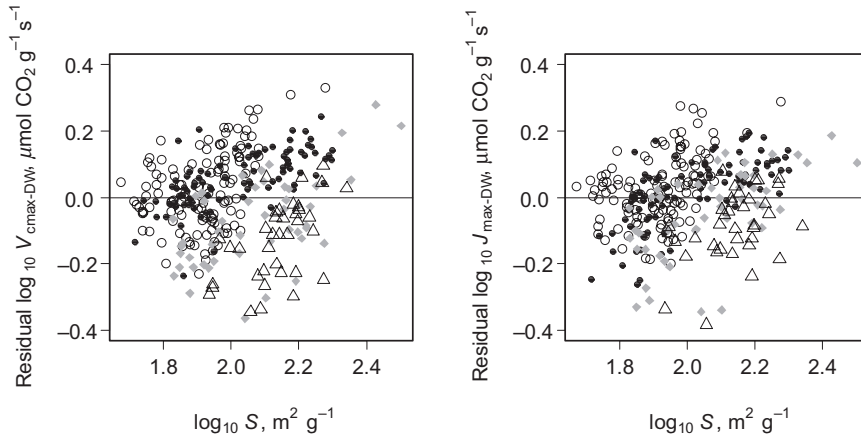


**Figure 6.** The influence of specific leaf area ( $S$ ) over Eqn 1 residuals ( $\log_{10}$  observation minus model prediction from Figure 5). Significant positive slopes of linear regression were observed for each vegetation group. Symbols are the same as in Figure 1.

density, such a result might be summarized as thinner leaves (low  $S$ ) being associated with higher nutrient use efficiencies. In addition, a shift in the N : P ratio where limitation changes from one nutrient to the other (i.e. the divide between blue and red dots on Fig. 7) was observed when the

data were grouped by  $S$ . For example, although the N : P ratio of high  $S$  leaves ( $133.4 \text{ cm}^2 \text{ g}^{-1}$ ; the mean  $S$  of the upper half of all  $S$  values) was equal to 15.1 for the  $V_{\text{cmax}}$  analysis (Fig. 7a), that ratio increased to 19.6 when a  $S$  equal to  $74.6 \text{ cm}^2 \text{ g}^{-1}$  (the mean  $S$  of the lower half of all  $S$  values)

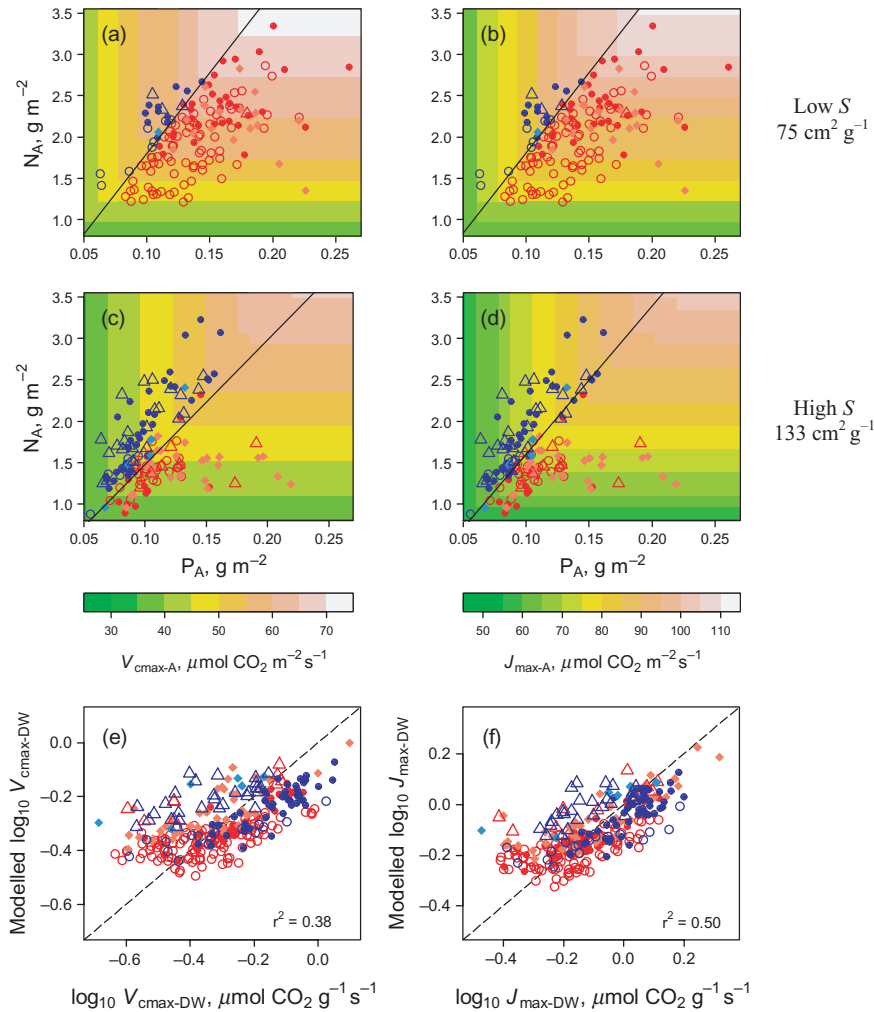


**Figure 7.** Predictions of photosynthetic capacity by Eqn 2 (color scale) when two average values of  $S$  were used. On graphs (a) and (b), mean  $S$  of the lower half of  $S$  values is used, whereas (c) and (d) utilizes mean  $S$  of the upper half. Blue and red symbols represent phosphorus and nitrogen limitations, respectively.  
 $\text{Log}_{10} V_{\text{cmax-DW}} = \min\{\alpha_N + v_N \log_{10} N + \sigma_N \log_{10} S, \alpha_P + v_P \log_{10} P + \sigma_P \log_{10} S\}$ , where  $\alpha_N = -1.56$ ;  $v_N = 0.43$ ;  $\sigma_N S = 0.37$ ;  $\alpha_P = -0.80$ ;  $v_P = 0.45$ ; and  $\sigma_P S = 0.25$ .  
 $\text{Log}_{10} J_{\text{max-DW}} = \min\{\gamma_N + \epsilon_N \log_{10} N + \zeta_N \log_{10} S, \gamma_P + \epsilon_P \log_{10} P + \zeta_P \log_{10} S\}$ , where  $\gamma_N = -1.50$ ;  $\epsilon_N = 0.41$ ;  $\zeta_N S = 0.45$ ;  $\gamma_P = -0.74$ ;  $\epsilon_P = 0.44$ ; and  $\zeta_P S = 0.32$ . Model performance is presented on panels (e) and (f). Symbols follow Figure 1 legend.

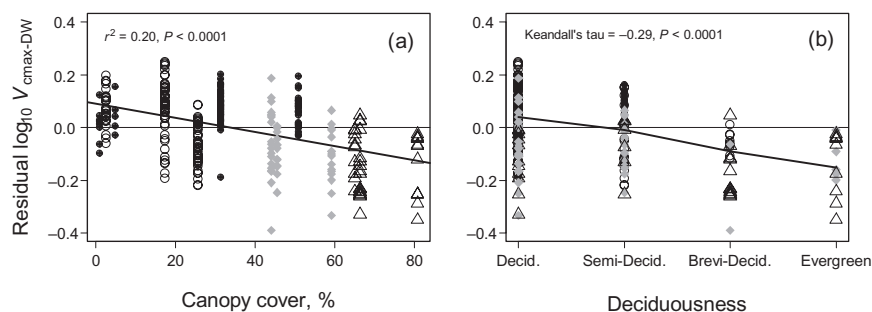


**Figure 8.** The significant effects of a quantitative (percent canopy cover) and qualitative (deciduousness) vegetation descriptors over Eqn 2 residuals ( $\log_{10}$  observation minus model predictions).

was used (Fig. 7c). The y-axis intercepts of the linear functions describing the four regression lines in Fig. 7 were always negative, although close to zero (average =  $-0.12 \text{ g m}^{-2} \text{ N}$ ). The improvement in model performance, when compared with Fig. 5 is illustrated in Fig. 7e, f.

Independent of which model was used, the vegetation types recognized in this study presented somewhat different relationships between photosynthetic capacity, leaf nutrient content and structure. Overall, these analyses demonstrate: (1) that S, N and P all play a role in explaining the observed variation in  $V_{\text{cmax}}$  and  $J_{\text{max}}$  in this west African data set (Fig. 2), but that the degree of influence for each term varies among the vegetation groups (Figs 3, 4, 6 and 7; Tables 2 and 3); (2) that the phosphorus constraint is larger for  $J_{\text{max}}$  than for  $V_{\text{cmax}}$  (Figs 5 and 7); and (3) that the N : P ratio that represents co-limitation of  $V_{\text{cmax}}$  and  $J_{\text{max}}$  varies non-linearly with  $N_{\text{DW}}$  (or  $P_{\text{DW}}$ ), and is distinct for  $V_{\text{cmax}}$  and  $J_{\text{max}}$  (Fig. 5), although it is strongly dependent on S, and becomes linear when this parameter is considered (Fig. 7).

In order to examine the validity of the new model, two independent tests were performed, one using an Amazon-wide data set and a second focusing at the stand scale. In the first, we applied the model to average leaf trait values reported for trees on fertile and infertile soils sampled across the Amazon Basin (Fyllas *et al.* 2009) in order to test whether Eqn 1 (Fig. 5) was able to replicate the substantial difference in the slope of the  $V_{\text{cmax}}\text{-N}$  relationship for low fertility oxisols (Ferralsols) and more fertile non-oxisols soils discussed by Kattge *et al.* (2009). In this test, the mean fertile soil values for  $N_{\text{DW}}$ ,  $P_{\text{DW}}$  and  $M_{\text{A}}$  were  $22.9 \text{ mg g}^{-1}$ ,  $1.27 \text{ mg g}^{-1}$  and  $98 \text{ g m}^{-2}$ , respectively, and the infertile soil values for  $N_{\text{DW}}$ ,  $P_{\text{DW}}$ ,  $M_{\text{A}}$ , which are classified as falling under strong phosphorus limitation according to Eqn 1 and Fig. 5, were  $20.6 \text{ mg g}^{-1}$ ,  $0.72 \text{ mg g}^{-1}$  and  $101 \text{ g m}^{-2}$ , respectively (data from Fyllas *et al.* 2009). Using these driving data, Eqn 1 yielded modelled  $V_{\text{cmax-A}}$  values for fertile and infertile soil of  $60.2$  and  $38.2 \mu\text{mol m}^{-2} \text{ s}^{-1}$ , respectively. Driving the separate models for oxisols and non-oxisols developed by Kattge *et al.* (2009) with the same N values, a very similar  $V_{\text{cmax-A}}$  value was obtained for oxisols ( $61.8 \mu\text{mol m}^{-2} \text{ s}^{-1}$ ), although  $V_{\text{cmax-A}}$  estimation for non-oxisol was slightly underestimated ( $28.4 \mu\text{mol m}^{-2} \text{ s}^{-1}$ ). This result is particularly encouraging given that all the vegetation sampled as part of this study in West Africa was growing on soils that would have been classified by

Quesada *et al.* (2009b) and Fyllas *et al.* (2009) as being in the 'fertile' category.

The second, more demanding test was for a single Amazonian site, for which a comparison of mass-based values was also possible. Using measurements of  $N_{\text{DW}}$ , S,  $V_{\text{cmax-DW}}$ ,  $J_{\text{max-DW}}$  and  $P_{\text{DW}}$  for canopy-top leaves from an eastern Amazonian rain forest (Domingues *et al.* 2007, with unpublished data provided for  $P_{\text{DW}}$ ) growing on a relatively infertile Ferralsol (oxisol) soil, Eqn 2 estimated  $V_{\text{cmax-DW}}$  to be  $0.45 \pm 0.09 \mu\text{mol g}^{-2} \text{ s}^{-1}$  (mean  $\pm$  SD), not significantly different from the measured average of  $0.39 \pm 0.16 \mu\text{mol g}^{-2} \text{ s}^{-1}$  (*t*-test assuming unequal variances, d.f. = 51,  $P = 0.1$ ). For  $J_{\text{max-DW}}$ , Eqn 2 estimated an average of  $0.69 \pm 0.15 \mu\text{mol g}^{-2} \text{ s}^{-1}$ , which was only marginally distinct (d.f. = 51,  $P = 0.07$ ) from the measurement derived value of  $0.60 \pm 0.22 \mu\text{mol g}^{-2} \text{ s}^{-1}$ . This exercise demonstrated that P limitation was prevailing, as 88% (23 out of 26) of the  $V_{\text{cmax-DW}}$  predictions and 85% of the  $J_{\text{max-DW}}$  were classified into this category by Eqn 2.

Finally, we noticed that some general vegetation descriptors had a significant influence over the residuals from the fits of Eqn 2 (Fig. 8), a strong suggestion of an apparent 'biome effect'. Similar patterns were also observed for plot-level LAI, basal area, or annual precipitation (not shown).

## DISCUSSION

### Global context

Leaf physical and chemical traits varied by up to fivefold over the study transect, presumably reflecting site differences in climate, leaf phenology, soil nutrient availability, species attributes and herbivory. Overall, the abundance of deciduous-habit species was negatively associated with precipitation leading to shorter-lived leaves with higher maximum photosynthetic capacities at the drier, lower-biomass sites (Fig. 1, Table 1, Appendix A), a result consistent with proposed leaf trait co-ordination strategies (Reich *et al.* 1997; Wright *et al.* 2004). However, leaf nutrient contents ( $N_{\text{DW}}$  and  $P_{\text{DW}}$ ) were not strongly correlated with mean annual precipitation (Table 1), and the clear contrasts reported for some Australian savannas (Wright *et al.* 2001; Prior *et al.* 2003) of low/high precipitation with associated high/low leaf nutrient content were not observed in this data set. This was, probably a reflection of inter-species

differences in leaf construction and, or, sample size, as well as variations in soil fertility associated with the wide range of different soil types sampled (Table 1).

For tropical woody savanna species, published  $A_{\text{sat}}$  ranges from 2.5 to 27  $\mu\text{mol m}^{-2} \text{s}^{-1}$  (Tuohy *et al.* 1991; Prado and de Moraes 1997; Hanan *et al.* 1998; Eamus *et al.* 1999; Wright *et al.* 2001; Prior *et al.* 2003; Midgley *et al.* 2004), similar to our results (5–28  $\mu\text{mol m}^{-2} \text{s}^{-1}$ ) that also included some forest species (Fig. 2). Far fewer estimates of photosynthetic capacity have been made in the tropics than in the temperate zone (Meir *et al.* 2007) but our data range ( $V_{\text{cmax}} = 20\text{--}90 \mu\text{mol m}^{-2} \text{s}^{-1}$ ;  $J_{\text{max}} = 30\text{--}140 \mu\text{mol m}^{-2} \text{s}^{-1}$ ) is similar to the majority of reported tropical values. For tropical forests and savannas,  $V_{\text{cmax}}$  (standardized to 25 °C) is generally 15–80  $\mu\text{mol m}^{-2} \text{s}^{-1}$  (e.g. Carswell *et al.* 2000; Coste *et al.* 2005; Domingues *et al.* 2005; Kenzo *et al.* 2006; Domingues *et al.* 2007; Meir *et al.* 2007), although some studies, where standardized leaf temperature was higher, and/or leaf nutrient concentrations were particularly large, have reported  $V_{\text{cmax}}$  values markedly higher than 120  $\mu\text{mol m}^{-2} \text{s}^{-1}$  (e.g. Midgley *et al.* 2004, Kenzo *et al.* 2006). In general, the relationship between  $J_{\text{max}}$  and  $V_{\text{cmax}}$  tends to be well defined, with a regression of  $J_{\text{max}}$  on  $V_{\text{cmax}}$  yielding a small positive  $J_{\text{max}}$  intercept and a slope of 1.3–1.7 (Wullschlegel 1993; Meir *et al.* 2002, 2007; Midgley *et al.* 2004; Coste *et al.* 2005). A marginally lower slope has been reported for South African savanna trees (1.3; Midgley *et al.* 2004) and this was also observed in our data (regression slope =  $1.2 \pm 0.03$  (standard error; inset, Fig. 1b). As it is not correct to consider  $V_{\text{cmax}}$  as a true independent variable when predicting  $J_{\text{max}}$ , analysis by SMA is probably more appropriate (Warton *et al.* 2006). Further, predicting  $J_{\text{max}}$  from  $V_{\text{cmax}}$  is not as informative as understanding how these two parameters scale with each other. Re-analysing the  $J_{\text{max}} - V_{\text{cmax}}$  relationship using SMA, a larger slope of 1.34 was returned, and the intercept decreased from 17.9 to 10.5  $\mu\text{mol m}^{-2} \text{s}^{-1}$  (linear SMA fits). Although every effort was made in this analysis to obtain unbiased fits to the Farquhar *et al.* (1980) model, the ratio of  $J_{\text{max}} : V_{\text{cmax}}$  varied slightly with the specific choice of model constants (see Methods) and species-specific interpretations probably require more detailed autecological physiology measurements to quantify parameters that were not included in this study, including mesophyll and intracellular conductances to  $\text{CO}_2$  ( $g_i$ ) (Warren 2008).

The bivariate contrasts of  $A_{\text{sat}}$  with  $M_A$ , N and P (Fig. 2) demonstrated wide variation within and among species and sites, even though significant regressions were still obtained. This scatter in the data probably reflected multiple ecological differences among species in: (1) the allocation of resources among structure, photosynthetic and non-photosynthetic compound pools (Poorter & Evans 1998; Hikosaka & Hirose 2000; Takashima *et al.* 2004; Harrison *et al.* 2009); (2) internal gas diffusion or light transmission constraints imposed by leaf structure (Lloyd *et al.* 1992; Parkhurst 1994; Green & Kruger 2001); and perhaps also (3) co-limitation by other nutrients (e.g. Güsewell 2004), although regressions involving leaf Mn, K, Ca, Al, Mg or S produced no significant interactions. The relationships in

our pooled data set deviate from those for a compiled global data set of leaf traits (Wright *et al.* 2004); the SMA slopes for all bivariate comparisons in Fig. 2 were significantly different from those reported by Wright *et al.* (2004). Separating the data by vegetation type and re-fitting SMA slopes showed that the low precipitation sites were the main cause of this variation (analysis not shown), reflecting both limitations in the global data set (cf. Niinemets *et al.* 2001) and perhaps the influence of the comparatively small sample size from our single study (Wright *et al.* 2006). This distinction among the vegetation groups was further underlined in the SMA slope analyses of  $V_{\text{cmax-A}}$  on  $N_A$  and  $P_A$  (Fig. 3).

### Leaf photosynthetic capacity, nitrogen and phosphorus

Photosynthetic capacity varied slightly more over the whole data set when expressed on a mass as opposed to an area basis (sevenfold versus fivefold), and both bivariate and multiple regressions of photosynthetic capacity on other leaf traits ( $M_A$ , or S, N and/or P) were stronger using mass-based comparisons (Table 2 and Appendix C), as has been reported elsewhere (e.g. Reich *et al.* 1997; Prior *et al.* 2003).  $V_{\text{cmax}}$  and  $J_{\text{max}}$  were more strongly related to  $N_{\text{DW}}$  than  $P_{\text{DW}}$ , except for SW trees. Although P has been hypothesized to strongly determine photosynthetic capacity in some savannas (e.g. Prior *et al.* 2003), wide variation elsewhere is evident (e.g. Tuohy *et al.* 1991; Wright *et al.* 2001; Meir *et al.* 2007). The best overall simple linear regression model structure in this study simply combined  $N_{\text{DW}}$  and S, but residual analysis demonstrated that site-specific multiple regression models incorporating  $P_{\text{DW}}$ , or sometimes removing  $N_{\text{DW}}$ , improved the estimates of  $V_{\text{cmax}}$  and  $J_{\text{max}}$  (Fig. 4). This underlines the differences along the transect in the principal driver of variation in  $V_{\text{cmax}}$  and  $J_{\text{max}}$ .

### Combining nitrogen and phosphorus constraints

A single representation of the influence of leaf structure ( $M_A$  or S) and leaf nutrient concentrations on photosynthetic capacity is clearly attractive for modelling purposes, and methods based on plant functional types (PFTs) have been developed for deriving global estimates of  $A_{\text{max}}$  (Reich *et al.* 2007) and  $V_{\text{cmax}}$  (Kattge *et al.* 2009). A substantial phosphorus constraint is, however, likely in many tropical forests (Vitousek & Sanford 1986; Lloyd *et al.* 2001; Hedin 2004; Reich & Oleksyn 2004; Quesada *et al.* 2009c), where separate relationships estimating  $V_{\text{cmax}}$  from N have been found necessary to account adequately for the large observed differences between tropical forests on soils with apparently low and high phosphorus availability (Kattge *et al.* 2009). The slope of the regression of  $V_{\text{cmax}}$  on  $N_A$  usually varies between 15 and 40  $\mu\text{mol CO}_2 \text{g}^{-1} \text{s}^{-1}$  (Kull 2002), but in several tropical rain forests, significantly lower values have been noted (Meir *et al.* 2007) and the data reported here are consistent with this pattern, with a mean

slope of  $17 \mu\text{mol CO}_2 \text{ g}^{-1} \text{ s}^{-1}$  for the pooled data set (based on non-transformed data). However we also note that the constraint by phosphorus on photosynthesis in tropical forests can be variable (Tuohy *et al.* 1991; Wright *et al.* 2001, 2006; Prior *et al.* 2003; Meir *et al.* 2007) and this reflects variation in species adaptation to both phosphorus and nitrogen acquisition, as well as to gradients in soil fertility and moisture availability. If, as it seems, these differences can be expressed at the leaf-level through divergent strategies in the allocation of N and P to photosynthetic and non-photosynthetic functions, some attractively simple stoichiometric analyses of N : P ratios (Sterner & Elser 2002) may ultimately be less informative than originally hoped, as has been noted elsewhere (Wright *et al.* 2006).

To represent the differential allocation of N and P to leaf function, separate models are required for each nutrient, which when combined, yield simultaneous independent constraints on photosynthetic capacity, with either N or P acting as the principal limiting nutrient on  $V_{\text{cmax}}$  (or  $J_{\text{max}}$ ) for any individual leaf. Both Eqns 1 and 2 represent this by assuming a simple linear model for each nutrient (cf. Kull 2002). As with the standard regression analyses, the best fits to Eqn 1 were obtained using mass-based leaf trait metrics, and indeed Eqn 1 performed better than all other standard regression models (Fig. 4, Table 4). The superiority in performance by Eqn 1 was marginal, but the result more informative and Fig. 5 illustrates how  $N_{\text{DW}}$  and  $P_{\text{DW}}$  co-limit  $V_{\text{cmax}}$  and  $J_{\text{max}}$  over the entire data set. Consistent with ecophysiological expectation, phosphorus was the limiting nutrient for  $J_{\text{max}}$  substantially more often than it was for  $V_{\text{cmax}}$  (45% versus 32% of all data points), with the reverse true for nitrogen (68% versus 55%). Such patterns are consistent with phosphorus limitation causing slight reductions in the  $J_{\text{max}}-V_{\text{cmax}}$  ratio (Fig. 1, inset), quite likely constraining carbon uptake at high irradiance and non-limiting soil moisture. The observed tendency for slight overestimation at low  $V_{\text{cmax-DW}}$  values and slight underestimation at high values was clearly related to vegetation type, as low  $V_{\text{cmax-DW}}$  values are associated with SDF vegetation whereas high values are dominated by OSS and OSW vegetation (Fig. 5c, d). This outcome results from the trade-off between having one general model versus a series of different models parameterized individually for each perceived vegetation type. Further, the pattern of these differences among vegetation types might also be influenced by the intrinsic functioning of the vegetation as a whole, as at the high end of our precipitation gradient, a decrease in deciduousness was observed (Appendix A). The increased discrepancy between observed and modelled photosynthetic capacity at higher  $S$  (Fig. 6) suggests that nutrient availability, phenology, and phylogeny, all exert a strong influence over  $S$  (Wright *et al.* 2004), and are influential parameters over primary productivity. This is further supported by Fig. 7, where the influence of  $S$  over photosynthetic capacity is presented. Interestingly, Eqn 2 predicts that thicker leaves are less susceptible to P-limitation, but achieve higher area-based photosynthetic capacity. Low  $S$  leaves have been associated previously with lower  $g_i$  (Lloyd *et al.* 1992;

Parkhurst 1994; Green & Kruger 2001), potentially leading to systematic errors in the estimations of  $V_{\text{cmax}}$  and  $J_{\text{max}}$  when this parameter is assumed to be infinite. Although it is still difficult to produce accurate estimates of  $g_i$  from curve fitting, we observed that 85% of the curves used here had  $g_i$  high enough (relative to  $A_{\text{sat}}$ ) to cause less than 20% of  $\text{CO}_2$  drawdown from the mesophyll to the carboxylation sites and concluded that the influence of this parameter on our data set was not significant. Furthermore, for this data set, there was no evidence of a positive association between  $S$  and  $g_i$ . Finally, as Eqn 2 allows N and P to scale independently with  $S$ , it accommodates the idea that nutrient pools not involved in photosynthesis might have very different sizes, for example, when a greater proportion of leaf N is allocated to cell walls in low  $S$  leaves (Poorter & Evans 1998; Hikosaka & Hirose 2000; Takashima *et al.* 2004; Harrison *et al.* 2009).

Overall, our unbalanced plot-level evaluation of general P-limitation revealed large natural variation ranging from no P-limitation at HOM-02 up to 100% P-limitation at ASU-01, with the extent of P-limitation increasing proportionally with plot-average leaf N : P ratio. As it stands, we recognize the possibility that different vegetation formations, with different nutrient dynamics and different phenological regimens may require adjustments to the parameters presented here in Eqns. 1 and 2 (Figs 5 and 7) to this West African data set.

A clear 'biome effect' was apparent in our analyses, as different vegetation types showed distinct characteristics in the photosynthesis – leaf trait relationships examined. The residuals from the fits of Eqn 2 were significantly correlated with general vegetation descriptors (Fig. 8). Clearly, the properties of the open canopy savannas differed from the closed canopy forests. Although a fully mechanistic understanding is not yet available, our observations could possibly be explained by a need for potentially large and readily mobile non-photosynthetic metabolic pools containing high amounts of N and/or P (e.g. as protein and/or mRNA). Such pools are thought to be more often necessary for fast adjustments of photosynthetic machinery for closed canopy species, which are often subject to large fluctuations in light regime because of competition from neighbouring trees or as a consequence of self-shading (Walters & Horton 1994; Walters 2005; Dietzel, Bräutigam & Pfannschmidt 2008). There is considerable variation in the degree to which different tropical tree species can acclimate to changes in light regime (Turnbull, Doley & Yates 1993; Rozendaal, Hurdato & Poorter 2006) and this might reflect a trade-off between an allocation of N and P for immediate photosynthetic carbon gain versus N and P being retained as reserve mRNA and protein precursors, should the need for photosynthetic acclimation arise. Consistent with this idea is the fact that pioneer species, when contrasted with climax species, tend to have not only higher rates of photosynthesis per unit N and, where examined, per unit P (Raaimeakers *et al.* 1995; Reich, Ellsworth & Uhl 1995; Rijkers, Pons & Bongers 2000), but are also associated with a lower ability to acclimate to variations in light regime (Rozendaal *et al.*

2006). Short-living pioneer species also tend to have low  $M_A$  and shorter leaf lifespans (Turner 2001), and indeed, generally speaking, it also seems intuitive that deciduous species, with short-lived leaves, would be less advantaged through investing some resources as insurance against a change in light regime (through non-photosynthetically active N and/or P) than would be the case for evergreen trees with longer-lived leaves. This postulate provides not only an explanation for the patterns observed between the model residuals and deciduousness in Fig. 8b, but also for the apparent contradiction between this study and that of Wright *et al.* (2001) who, working in New South Wales, Australia, found that N and P, although expressed on a dry-weight basis, seemed to be used less efficiently for low-rainfall species growing in an aseasonal rainfall environment than for those from high-rainfall species – this being the opposite result to that found here (Fig. 2). This may be because all species examined in Wright *et al.* (2001) were evergreen (Ian Wright, personal communication) as opposed to the predominately deciduous species encountered in the present study. Similar lifespans are commonly observed for evergreen leaves from both dry and moist habitats (Wright & Westoby 2002; Wright *et al.* 2005b), although increased leaf longevity in moist habitats is not necessarily related to higher  $M_A$  as observed for evergreen tree species in drier habitats (Specht & Specht 1989). Furthermore, evergreen leaves from dry habitats are often exposed to periods of mild-to severe soil water deficits especially as xeromorphic trees and shrubs are usually found in aseasonal precipitation environments characterized by episodic precipitation events (Lloyd & Farquhar 1994). This suggests that leaves in such climates (as was the case for Wright *et al.* 2001) might be advantaged by allocating some of their N and/or P away from short-term photosynthetic carbon gain to allow for the involvement of N- and P-containing compounds in drought induced metabolic pathways, including, amongst others, late embryogenesis abundant (LEA) proteins, mRNA binding proteins, water channel proteins, detoxification enzymes, transcription factors, protein kinases, protein phosphatases and enzymes involved in phospholipid metabolism (Boudsocq & Laurière 2005; Shinozaki & Yamaguchi-Shinozaki 2007). On the other hand, drought-deciduous trees tend to occur in environments characterized by a regular seasonal water supply (Lloyd & Farquhar 1994) – as was the case in the present study – and, because of the less likelihood of severe soil water deficits occurring during the growing season, are also characterized by an aggressive water use strategy (Lloyd & Farquhar 1994). An allocation of the bulk of N and P to the photosynthetic apparatus (rather than as N- and P-containing precursor compounds should drought induced metabolic pathways need to be activated) would thus be expected in such a situation with the proportion allocated to non-photosynthetic pathways declining with shorter growing seasons and hence lower leaf lifetimes thus consistent with the generally higher photosynthetic rates per unit N for the more open drier vegetation with shorter leaf lifespans (Figs 5, 7 and 8). Indeed, one subtlety in the data,

that being that OSW rather than OSS leaves tend to have the highest rates of  $A$  per unit N or P (Figs 2 and 3) and with the most severely underestimated values for  $V_{\text{cmax}}$  and  $J_{\text{max}}$  compared with model predictions (Figs 5–7) is also explained by the hypothesis mentioned earlier. This is because the bulk of the precipitation in the Sahel occurs during a small number of line squalls, with these being highly variable in frequency and precipitation intensity and with a strong year-to-year variability (Hayward & Oguntoyinbo 1987). It is therefore likely that, in contrast to the OSW vegetation further south, that leaves of OSS are often exposed to severe water deficits, even during the relatively short wet season. According to the above theory, they would therefore be expected to allocate more of their N and P to potentially activated drought metabolic pathways than for the OSW vegetation with more reliable rainfall patterns further south; and hence with a lower rate of photosynthesis per unit bulked leaf N or P.

The availability of data from tropical vegetation that is suitable to test the proposed models is limited. However, we note that by combining Eqn 1 with  $M_A$  and testing at a very large scale, the estimates for  $V_{\text{cmax}}$  and  $J_{\text{max}}$  matched the generalized differences in  $V_{\text{cmax}}$  and  $J_{\text{max}}$  expected for fertile and non-fertile tropical soils and previously attributed to low and high foliar P concentrations, respectively (Fyllas *et al.* 2009; Kattge *et al.* 2009). Furthermore, Eqn 2 successfully predicted independent observations from a potentially P-limited rain-forest (N : P ratio = 24). The wide availability and low data acquisition cost of  $M_A$ , N and P for different vegetation types (Reich *et al.* 2007) make this a promising step forward in trying to unravel and generalize the roles of nitrogen and phosphorus in determining photosynthetic capacity in tropical woody vegetation, a still poorly explored but important research frontier in global ecophysiology.

## CONCLUSIONS

This study presents substantial new combined leaf trait and photosynthesis measurements to address the scarcity of such data for tropical forests and savannas. Although our results are broadly consistent with existing global patterns in leaf traits governing  $A_{\text{sat}}$ ,  $M_A$ , N and P (Wright *et al.* 2004), differences from these global patterns are evident (Fig. 2). Despite being required for vegetation models, estimates of  $V_{\text{cmax}}$  and  $J_{\text{max}}$  are scarce for tropical ecosystems (Xu *et al.* 2009) and our values are consistent with reported measurements in rain forests and savanna, especially with the peculiarly low slope for the regression of  $V_{\text{cmax}}$  on  $N_A$  observed elsewhere (Meir *et al.* 2007). In a new model framework that simultaneously fits independent linear relationships for both N and P with  $V_{\text{cmax}}$  and  $J_{\text{max}}$  we show that it is possible to improve on standard multiple regression approaches and we indicate the potential for a single general model of N and P limitation on the photosynthesis of tropical vegetation. This model performs well when tested against the limited data available and can be further refined and improved as more tropical forest and savanna

data sets across a wider range of climates and soil types become available.

## ACKNOWLEDGMENTS

Many people provided invaluable help during this work. Field work assistance was provided by Michael Schwarz, Markus Fink, and Prof Oliver Philips and we thank Dr Eric Mougin and colleagues for their hospitality and assistance while in Mali. The Forest Research Institute of Ghana (FORIG) provided vehicles, drivers (Simon, Samuel and Osei), botanists (Mr Ntin and Mr Tony), local support (Kester), and lab space. The Scientific Research Station of the Dreyer Foundation in Dano provided excellent accommodations and support with Wareh Zakaria helping with plant identification and field assistance at Mole. Martin Gilpin overviewed lab analyses, and Dr David Harris helped with species deciduousness classification. This work was funded as part of the UK National Environment Research Council Tropical Biomes in Transition (TROBIT) consortium via research grant NE/D01185x/1 to the University of Edinburgh.

## REFERENCES

- Akaike H. (1974) A new look at the statistical model identification. *IEEE Transactions on Automatic Control* **19**, 716–723.
- Beerling D.J. & Quick W.P. (1995) A new technique for estimating rates of carboxylation and electron-transport in leaves of C-3 plants for use in dynamic global vegetation models. *Global Change Biology* **1**, 289–294.
- Bernacchi C.J., Pimentel C. & Long S.P. (2003) In vivo temperature response functions of parameters required to model RuBP-limited photosynthesis. *Plant, Cell & Environment* **26**, 1419–1430.
- Boudsocq M. & Laurière C. (2005) Osmotic signaling in plants. Multiple pathways mediated by emerging kinase families. *Plant Physiology* **138**, 1185–1194.
- Burnham K.P. & Anderson D.R. (2002) *Model Selection and Multimodel Inference: A Practical-Theoretic Approach*, 2nd edn, Springer-Verlag, Fort Collins, CO, USA.
- von Caemmerer S. (2000) *Biochemical Model of Leaf Photosynthesis*, pp. 1–165. SCIRO Publishing, Collingwood, Victoria, Australia.
- Carswell F.E., Meir P., Wandelli E.V., Bonates L.C.M., Kruijt B., Barbosa E.M., Nobre A.D., Grace J. & Jarvis P.G. (2000) Photosynthetic capacity in a central Amazonian rain forest. *Tree Physiology* **20**, 179–186.
- Coste S., Roggy J.C., Imbert P., Born C., Bonal D. & Dreyer E. (2005) Leaf photosynthetic traits of 14 tropical rain forest species in relation to leaf nitrogen concentration and shade tolerance. *Tree Physiology* **25**, 1127–1137.
- Dietzel L., Bräutigam K. & Pfannschmidt T. (2008) Photosynthetic acclimation: State transitions and adjustment of photosystem stoichiometry – functional relationships between short-term and long-term light quality acclimation in plants. *FEBS Journal* **275**, 1080–1088.
- Domingues T.F., Berry J.A., Martinelli L.A., Ometto J.P.H. & Ehleringer J.R. (2005) Parameterization of canopy structure and leaf-level gas exchange for an eastern Amazonian tropical rain forest (Tapajós National Forest, Pará, Brazil). *Earth Interactions* **9**, 1–23.
- Domingues T.F., Martinelli L.A. & Ehleringer J.R. (2007) Eco-physiological traits of plant functional groups in forest and pasture ecosystems from eastern Amazônia, Brazil. *Plant Ecology* **193**, 101–112.
- Eamus D., Myers B., Duff G. & Williams D. (1999) Seasonal changes in photosynthesis of eight savanna tree species. *Tree Physiology* **19**, 665–671.
- Evans J.R. (1989) Photosynthesis and nitrogen relationships in leaves of C<sub>3</sub> plants. *Oecologia* **78**, 9–19.
- Farquhar G.D., von Caemmerer S. & Berry J.A. (1980) A biochemical model of photosynthetic CO<sub>2</sub> assimilation in leaves of C<sub>3</sub> species. *Planta* **149**, 78–90.
- Field C.B. & Mooney H.A. (1986) The photosynthesis-nitrogen relationship in wild plants. In *On the Economy of Plant Form and Function* (ed. T.J. Givnish), pp. 25–55. Cambridge University Press, Cambridge.
- Franco A.C. (1998) Seasonal patterns of gas exchange, water relations and growth of *Roupala montana*, an evergreen savanna species. *Plant Ecology* **136**, 69–76.
- Furley P.A. (1992) Edaphic changes at the forest-savanna boundary with particular reference to the neotropics. In *Nature and Dynamics of Forest-Savanna Boundaries* (eds P.A. Furley, J. Proctor & J.A. Ratter), pp. 91–117. Chapman & Hall, London.
- Fyllas N.M., Patiño S., Baker T.R., et al. (2009) Basin-wide variations in foliar properties of Amazonian forest: phylogeny, soils and climate. *Biogeosciences Discussions* **6**, 3707–3769.
- Gifford R.M. & Evans L.T. (1981) Photosynthesis, carbon partitioning, and yield. *Annual Review of Plant Physiology and Plant Molecular Biology* **32**, 485–509.
- Green D.S. & Kruger E.L. (2001) Light-mediated constraints on leaf function correlate with leaf structure among deciduous and evergreen tree species. *Tree Physiology* **21**, 1341–1346.
- Güsewell S. (2004) N : P ratios in terrestrial plants: variation and functional significance. *New Phytologist* **164**, 243–266.
- Hanan N.P., Kabat P., Dolman A.J. & Elbers J.A. (1998) Photosynthesis and carbon balance of a Sahelian fallow savanna. *Global Change Biology* **4**, 523–538.
- Harley P.C., Thomas R.B., Reynolds J.F. & Strain B.R. (1992) Modelling photosynthesis of cotton grown in elevated CO<sub>2</sub>. *Plant, Cell & Environment* **15**, 271–282.
- Harrison M.T., Edwards E.J., Farquhar G.D., Nicotra A.B. & Evans J.R. (2009) Nitrogen in cell walls of sclerophyllous leaves accounts for little of the variation in photosynthetic nitrogen-use efficiency. *Plant, Cell & Environment* **32**, 259–270.
- Hayward D. & Oguntoyinbo J. (1987) *The Climatology of West Africa*. Century Hutchinson, London, 271p.
- Hedin L.O. (2004) Global organization of terrestrial plant-nutrient interactions. *Proceedings of the National Academy of Sciences of the United States of America* **101**, 10849–10850.
- Hikosaka K. & Hirose T. (2000) Photosynthetic nitrogen-use efficiency in evergreen broad-leaved woody species coexisting in a warm-temperate forest. *Tree Physiology* **20**, 1249–1254.
- Högberg P. (1986) Soil nutrient availability, root symbioses and tree species composition in tropical Africa: A review. *Journal of Tropical Ecology* **2**, 359–372.
- IUSS (International Union of Soil Science) Working Group WRB (2006) *World Reference Base for Soil Resources 2006: A Framework for International Classification, Correlation and Communication*. World Soil Resources Report 103, FAO, Rome.
- Kattge J., Knorr W., Raddatz T. & Wirth C. (2009) Quantifying photosynthetic capacity and its relationship to leaf nitrogen content for global-scale terrestrial biosphere models. *Global Change Biology* **15**, 976–991.
- Keay R.W.J. (1949) An example of Sudan zone vegetation in Nigeria. *The Journal of Ecology* **37**, 335–364.

- Kenzo T., Ichie T., Watanabe Y., Yoneda R., Ninomiya I. & Koike T. (2006) Changes in photosynthesis and leaf characteristics with tree height in five dipterocarp species in a tropical rain forest. *Tree Physiology* **26**, 865–873.
- Kull O. (2002) Acclimation of photosynthesis in canopies: models and limitations. *Oecologia* **133**, 267–279.
- Lambers H., Raven J.A., Shaver G.R. & Smith S.E. (2008) Plant nutrient-acquisition strategies change with soil age. *Trends in Ecology and Evolution* **23**, 95–103.
- Lloyd J. & Farquhar G.D. (1994)  $^{13}\text{C}$  discrimination during  $\text{CO}_2$  assimilation by the terrestrial biosphere. *Oecologia* **99**, 201–215.
- Lloyd J., Syvertsen J.P., Kriedemann P.E. & Farquhar G.D. (1992) Low conductances for  $\text{CO}_2$  diffusion from stomata to the sites of carboxylation in leaves of woody species. *Plant, Cell & Environment* **15**, 873–899.
- Lloyd J., Bird M.I., Veenendaal E.M. & Kruijt B. (2001) Should phosphorus availability be constraining moist tropical forest responses to increasing  $\text{CO}_2$  concentration. In *Global Biogeochemical Cycles in the Climate System* (eds E.-D. Schulze, M. Heimann, S. Harrison, E. Holland, J. Lloyd, I.C. Prentice & D. Schimel), p. 350. Academic Press, London, UK.
- Lloyd J., Bird M.I., Vellen L., Miranda A.C., Veenendaal E.M., Djagbletey G., Miranda H.S., Cook G. & Farquhar G.D. (2008) Contributions of woody and herbaceous vegetation to tropical savanna ecosystem productivity: a quasi-global estimate. *Tree Physiology* **28**, 451.
- Lloyd J., Goulden M., Ometto J.P., Fyllas N.M., Quesada C.A. & Patiño S. (2009) Ecophysiology of forest and savanna vegetation. In *Amazonia and Climate Change* (eds M. Keller, J. Gash & P. Silva Dias), pp. 463–484. American Geophysical Union, Washington, DC, USA.
- Long S.P. & Bernacchi C.J. (2003) Gas exchange measurements, what can they tell us about the underlying limitations to photosynthesis? Procedures and sources of error. *Journal of Experimental Botany* **54**, 2393–2401.
- Mardegan S.F., Nardoto G.B., Higuchi N., Moreira M.Z. & Martinelli L.A. (2008) Nitrogen availability patterns in white-sand vegetations of Central Brazilian Amazon. *Trees – Structure and Function* **23**, 479–488.
- Martinelli L.A., Piccolo M.C., Townsend A.R., Vitousek P.M., Cuevas E., McDowell W., Robertson G.P., Santos O.C. & Treseder K. (1999) Nitrogen stable isotopic composition of leaves and soil: Tropical versus temperate forests. *Biogeochemistry* **46**, 45–65.
- Meir P., Grace J. & Miranda A.C. (2001) Leaf respiration in two tropical rainforests: constraints on physiology by phosphorus, nitrogen and temperature. *Functional Ecology* **15**, 378–387.
- Meir P., Kruijt B., Broadmeadow M., Barbosa E., Kull O., Carswell F.E., Nobre A. & Jarvis P.G. (2002) Acclimation of photosynthetic capacity to irradiance in tree canopies in relation to leaf nitrogen concentration and leaf mass per unit area. *Plant, Cell & Environment* **25**, 343–357.
- Meir P., Levy P., Grace J. & Jarvis P. (2007) Photosynthetic parameters from two contrasting woody vegetation types in West Africa. *Plant Ecology* **192**, 277–287.
- Midgley G.F., Aranibar J.N., Mantlana K.B. & Macko S. (2004) Photosynthetic and gas exchange characteristics of dominant woody plants on a moisture gradient in an African savanna. *Global Change Biology* **10**, 309–317.
- Mooney H.A., Field C., Gulmon S.L., Rundel P. & Kruger F.J. (1983) Photosynthetic characteristic of South-African sclerophylls. *Oecologia* **58**, 398–401.
- New M., Hulme M. & Jones P. (1999) Representing twentieth-century space-time climate variability. Part I: Development of a 1961–90 mean monthly terrestrial climatology. *Journal of Climate* **12**, 829–856.
- Niinemets Ü. (1999) Components of leaf dry mass per area – thickness and density – alter leaf photosynthetic capacity in reverse directions in woody plants. *New Phytologist* **144**, 35–47.
- Niinemets Ü., Ellsworth D.S., Lukjanova A. & Tobias M. (2001) Site fertility and the morphological and photosynthetic acclimation of *Pinus sylvestris* needles to light. *Tree Physiology* **21**, 1231–1244.
- Nocedal J. & Wright S.J. (2006) *Numerical Optimization* 2nd edn, Springer, New York.
- Okin G.S., Mladenov N., Wang L., Cassel D., Caylor K.K., Ringrose S. & Macko S.A. (2008) Spatial patterns of soil nutrients in two southern African savannas. *Journal of Geophysical Research* **113**, G02011. DOI: 10.1029/2007JG000584.
- Ollinger S. & Smith M.-L. (2005) Net primary production and canopy nitrogen in a temperate forest landscape: An analysis using imaging spectroscopy, modeling and field data. *Ecosystems* **8**, 760–778.
- Paoli G.D. & Curran L.M. (2007) Soil nutrients limit fine litter production and tree growth in mature low-land forest of South-western Borneo. *Ecosystems* **10**, 503–518.
- Parkhurst D.F. (1994) Diffusion of  $\text{CO}_2$  and other gases inside leaves. *New Phytologist* **126**, 449–479.
- Poorter H. & Evans J.R. (1998) Photosynthetic nitrogen-use efficiency of species that differ inherently in specific leaf area. *Oecologia* **116**, 26–37.
- Prado C.H.B. & de Moraes J.A.P.V. (1997) Photosynthetic capacity and specific leaf mass in twenty woody species of Cerrado vegetation under field conditions. *Photosynthetica* **33**, 103–112.
- Prior L.D., Eamus D. & Bowman D.M.J. (2003) Leaf attributes in the seasonally dry tropics: a comparison of four habitats in northern Australia. *Functional Ecology* **17**, 504–515.
- Quesada C.A., Lloyd J., Anderson L.O., Fyllas N.M., Schwarz M. & Czimczik C.I. (2009a) Soils of Amazonia with particular reference to the RAINFOR sites. *Biogeosciences Discussions* **6**, 3851–3921.
- Quesada C.A., Lloyd J., Schwarz M., et al. (2009b) Chemical and physical properties of Amazon forest soils in relation to their genesis. *Biogeosciences Discussions* **6**, 3923–3992.
- Quesada C.A., Lloyd J., Schwarz M., et al. (2009c) Regional and large-scale patterns in Amazon forest structure and function are mediated by variations in soil physical and chemical properties. *Biogeosciences Discussions* **6**, 3993–4057.
- R Development Core Team (2008) R: A language and environment for statistical computing. R Foundation for Statistical Computing, Vienna, Austria. ISBN 3-900051-07-0, URL: <http://www.R-project.org>.
- Raaimakers D., Boot R.G.A., Dijkstra P., Pot S. & Pons T. (1995) Photosynthetic rates in relation to leaf phosphorus content in pioneer versus climax tropical forest trees. *Oecologia* **102**, 120–125.
- Raddatz T.J., Reick C.H., Knorr W., Kattge J., Roegner E., Schnur R., Schnitzler K.G., Wetzel P. & Jungclaus J. (2007) Will the tropical land biosphere dominate the climate-carbon cycle feedback during the twenty-first century? *Climate Dynamics* **29**, 565–574.
- Reich P.B. & Oleksyn J. (2004) Global patterns of plant leaf N and P in relation to temperature and latitude. *Proceedings of the National Academy of Sciences of the United States of America* **101**, 11001–11006.
- Reich P.B., Ellsworth D.S. & Uhl C. (1995) Leaf carbon and nutrient assimilation in species of differing successional status in an oligotrophic Amazonian forest. *Functional Ecology* **9**, 65–76.
- Reich P.B., Ellsworth D.S., Walters M.B., Vose J.M., Gresham C., Volin J.C. & Bowman W.D. (1999) Generality of leaf trait relationships: a test across six biomes. *Ecology* **80**, 1955–1969.
- Reich P.B., Hobbie S.E., Lee T., Ellsworth D.S., West J.B., Tilman

- D., Knops J.M.H., Naeem S. & Trost J. (2006) Nitrogen limitation constrains sustainability of ecosystem response to CO<sub>2</sub>. *Nature* **440**, 922–925.
- Reich P.B., Oleksyn J. & Wright I. (2009) Leaf phosphorus influences the photosynthesis-nitrogen relation: a cross-biome analysis of 314 species. *Oecologia* **160**, 207–212.
- Reich P.B. & Schoettle A.W. (1988) Role of phosphorus and nitrogen in photosynthetic and whole plant carbon gain and nutrient use efficiency in eastern white-pine. *Oecologia* **77**, 25–33.
- Reich P.B., Walters M.B. & Ellsworth D.S. (1997) From tropics to tundra: global convergence in plant functioning. *Proceedings of the National Academy of Sciences* **94**, 13730–13734.
- Reich P.B., Wright I.J. & Lusk C.H. (2007) Predicting leaf physiology from simple plant and climate attributes: a global GLOPNET analysis. *Ecological Applications* **17**, 1982–1988.
- Rijkers T., Pons T.L. & Bongers F. (2000) The effect of tree height and light availability on photosynthetic leaf traits of four neotropical species differing in shade tolerance. *Functional Ecology* **14**, 77–86.
- Rozendaal D.M.A., Hurdato V.H. & Poorter L. (2006) Plasticity in leaf traits of 38 tropical tree species in response to light; relationship with light demand and adult stature. *Functional Ecology* **20**, 207–216.
- Santiago L.S. & Mulkey S.S. (2003) A test of gas exchange measurements on excised canopy branches of ten tropical tree species. *Photosynthetica* **41**, 343–347.
- Schulze E.-D., Kelliher F.M., Korner C., Lloyd J. & Leuning R. (1994) Relationships among maximum stomatal conductance, ecosystem surface conductance, carbon assimilation rate, and plant nitrogen nutrition: A global ecology scaling exercise. *Annual Review of Ecology and Systematics* **25**, 629–660.
- Sellers P.J., Dickinson R.E., Randall D.A., *et al.* (1997) Modeling the exchanges of energy, water, and carbon between continents and the atmosphere. *Science* **275**, 502–509.
- Shinozaki K. & Yamaguchi-Shinozaki K. (2007) Gene networks involved in drought stress response and tolerance. *Journal of Experimental Botany* **58**, 221–227.
- Sitch S., Smith B., Prentice I.C., *et al.* (2003) Evaluation of ecosystem dynamics, plant geography and terrestrial carbon cycling in the LPJ dynamic global vegetation model. *Global Change Biology* **9**, 161–185.
- Specht R.L. & Specht A. (1989) Canopy structure in *Eucalyptus* dominated communities in Australia along climatic gradients. *Acta Oecologia, Oecologia Plantarum* **10**, 191–213.
- Sterner R.W. & Elser J.J. (2002) *Ecological Stoichiometry: The Biology of Elements from Molecules to the Biosphere*. Princeton University Press, 584p.
- Takashima T., Hikosaka K. & Hirose T. (2004) Photosynthesis or persistence: nitrogen allocation in leaves of evergreen and deciduous *Quercus* species. *Plant, Cell & Environment* **27**, 1047–1054.
- Terashima I., Araya T., Miyazawa S.-I., Sone K. & Yano S. (2005) Construction and maintenance of the optimal photosynthetic systems of the leaf, herbaceous plant and tree: an eco-developmental treatise. *Annals of Botany* **95**, 507–519.
- Tjellström H., Andersson M.X., Larsson K.E. & Sandelius A.S. (2008) Membrane phospholipids as a phosphate reserve: the dynamic nature of phospholipid-to-digalactosyl diacylglycerol exchange in higher plants. *Plant, Cell & Environment* **31**, 1388–1398.
- Tuohy J.M., Prior J.A.B. & Stewart G.R. (1991) Photosynthesis in relation to leaf nitrogen and phosphorus-content in Zimbabwean trees. *Oecologia* **88**, 378–382.
- Turnbull M.H., Doley D. & Yates D.J. (1993) The dynamics of photosynthetic acclimation to changes in light quantity and quality in three Australian rainforest tree species. *Oecologia* **94**, 218–228.
- Turner I.M. (2001) *The Ecology of Trees in the Tropical Rain Forest*. Cambridge University Press, Cambridge, 298p.
- Vitousek P.M. & Sanford Jr R.L. (1986) Nutrient cycling in moist tropical forest. *Annual Review of Ecology and Systematics* **17**, 137–167.
- Walters R.G. (2005) Towards an understanding of photosynthetic acclimation. *Journal of Experimental Botany* **56**, 435–447.
- Walters R.G. & Horton P. (1994) Acclimation of *Arabidopsis thaliana* to the light environment: Changes in composition of the photosynthetic apparatus. *Planta* **195**, 248–256.
- Warren C.R. (2008) Stand aside stomata, another actor deserves centre stage: the forgotten role of the internal conductance to CO<sub>2</sub> transfer. *Journal of Experimental Botany* **59**, 1475–1487.
- Warton D.I., Wright I.J., Falster D.S. & Westoby M. (2006) Bivariate line-fitting methods for allometry. *Biological Reviews* **81**, 259–291.
- White F. (1983) *The Vegetation of Africa: A Descriptive Memoir to Accompany the UNESCO/AETFAT/UNSO Vegetation Map of Africa*. UNESCO, Paris, 356p.
- Woodrow I.E. & Berry J.A. (1988) Enzymatic regulation of photosynthetic CO<sub>2</sub> fixation in C<sub>3</sub> plants. *Annual Review of Plant Physiology and Plant Molecular Biology* **39**, 533–594.
- Woodward F.I., Smith T.M. & Emanuel W.R. (1995) A global land primary productivity and phytogeography model. *Global Biogeochemical Cycles* **9**, 471–490.
- Wright I.J. & Westoby M. (2002) Leaves at low versus high rainfall: coordination of structure, lifespan and physiology. *New Phytologist* **155**, 403–416.
- Wright I.J., Reich P.B. & Westoby M. (2001) Strategy shifts in leaf physiology, structure and nutrient content between species of high- and low-rainfall and high- and low-nutrient habitats. *Functional Ecology* **15**, 423–434.
- Wright I.J., Reich P.B., Westoby M., *et al.* (2004) The worldwide leaf economics spectrum. *Nature* **428**, 821.
- Wright I.J., Reich P.B., Cornelissen J.H.C., *et al.* (2005a) Assessing the generality of global leaf trait relationships. *New Phytologist* **166**, 485–496.
- Wright I.J., Reich P.B., Cornelissen J.H.C., *et al.* (2005b) Modulation of leaf economic traits and trait relationships by climate. *Global Ecology and Biogeography Letters* **14**, 411–421.
- Wright I.J., Leishman M.R., Read C. & Westoby M. (2006) Gradients of light availability and leaf traits with leaf age and canopy position in 28 Australian shrubs and trees. *Functional Plant Biology* **33**, 407–419.
- Wullschlegel S.D. (1993) Biochemical limitations to carbon assimilation in C<sub>3</sub> plants. A retrospective analysis of the A/Ci curves from 109 species. *Journal of Experimental Botany* **44**, 907–920.
- Xu C., Gertner G.Z. & Scheller R.M. (2009) Uncertainties in the response of a forest landscape to global climatic change. *Global Change Biology* **15**, 116–131.

Received 10 October 2009; received in revised form 8 January 2010; accepted for publication 11 January 2010

## APPENDIX A

Table A1. Summary of species sampled at each region and their averages of parameters evaluated. Values are mean  $\pm$  standard deviation when number of individuals sampled is >1

Plot	Species	Phenology	Individuals (total replicates)	Leaf thickness (mm)	$M_A$ (g m <sup>-2</sup> )	$A_{site}^A$ ( $\mu\text{molCO}_2$ m <sup>-2</sup> s <sup>-1</sup> )	$V_{max}^A$ ( $\mu\text{molCO}_2$ m <sup>-2</sup> s <sup>-1</sup> )	$J_{max}^A$ ( $\mu\text{molCO}_2$ m <sup>-2</sup> s <sup>-1</sup> )	$N^A$ (g m <sup>-2</sup> )	$P^A$ (g m <sup>-2</sup> )
HOM-01	<i>Acacia senegal</i> Willd	D <sup>a</sup>	1 (1)	0.34	65.3 $\pm$ 0	21.6 $\pm$ 0	73.6 $\pm$ 0	99.6 $\pm$ 0	3.06 $\pm$ 0	0.162 $\pm$ 0
HOM-01	<i>Combretum glutinosum</i> Perr. Ex DC.	D <sup>a</sup>	3 (9)	0.5 $\pm$ 0.03	156 $\pm$ 11.5	19.2 $\pm$ 1.5	69.2 $\pm$ 6.6	91.7 $\pm$ 8.8	2.63 $\pm$ 0.49	0.18 $\pm$ 0.035
HOM-02	<i>Combretum glutinosum</i> Perr. Ex DC.	D <sup>a</sup>	1 (3)		139.9	19.3	64	69	2.29	0.152
BBI-01	<i>Acacia gournaiensis</i> A.Chev.	D <sup>c</sup>	3 (9)		72.9 $\pm$ 10.1	18.7 $\pm$ 4.1	61 $\pm$ 11.8	83.4 $\pm$ 16.1	1.93 $\pm$ 0.44	0.11 $\pm$ 0.027
BBI-01	<i>Anogeissus leiocarpus</i> Guill. & Perr.	D <sup>a</sup>	3 (15)		62.3 $\pm$ 4.7	10.6 $\pm$ 2.5	49.4 $\pm$ 2.9	72.8 $\pm$ 9	1.25 $\pm$ 0.13	0.093 $\pm$ 0.013
BBI-01	<i>Combretum glutinosum</i> Perr. Ex DC.	D <sup>a</sup>	3 (18)		131 $\pm$ 9.7	19 $\pm$ 2.3	69.1 $\pm$ 6.4	97.4 $\pm$ 12.2	2.35 $\pm$ 0.2	0.158 $\pm$ 0.019
BBI-01	<i>Combretum micranthum</i> G. Don	D <sup>a</sup>	3 (12)		73.6 $\pm$ 10.5	14.3 $\pm$ 6	60.1 $\pm$ 13.8	87.5 $\pm$ 21.9	2.07 $\pm$ 0.63	0.115 $\pm$ 0.03
BBI-02	<i>Acacia dregeana</i> Craib	D <sup>a</sup>	3 (8)		78.9 $\pm$ 16.2	19 $\pm$ 4.2	63.9 $\pm$ 16.6	92.7 $\pm$ 18.4	2.27 $\pm$ 0.57	0.104 $\pm$ 0.02
BBI-02	<i>Lannea acida</i> A.Rich.	D <sup>a</sup>	3 (9)		107.1 $\pm$ 12	17.3 $\pm$ 0.4	55.2 $\pm$ 1	87 $\pm$ 6.7	1.88 $\pm$ 0.13	0.106 $\pm$ 0.01
BBI-02	<i>Vitellaria paradoxa</i> C.F. Gaertn.	SD <sup>a</sup>	3 (9)		132 $\pm$ 14.5	19.2 $\pm$ 3.1	67.9 $\pm$ 8.9	103.1 $\pm$ 12.5	2.36 $\pm$ 0.23	0.12 $\pm$ 0.015
BDA-01	<i>Cochlospermum planchoni</i> Hook.f. ex Planch.	D <sup>f</sup>	3 (8)	0.32 $\pm$ 0.01	86.1 $\pm$ 4.1	19 $\pm$ 5	66.5 $\pm$ 11	92.3 $\pm$ 15.7	1.45 $\pm$ 0.08	0.114 $\pm$ 0.009
BDA-01	<i>Daniellia oliveri</i> Hutch. & Dalziel.	D <sup>a</sup>	3 (9)	0.32 $\pm$ 0.02	109.2 $\pm$ 6.9	19.7 $\pm$ 1.2	64 $\pm$ 4	90.9 $\pm$ 6.7	1.67 $\pm$ 0.26	0.114 $\pm$ 0.013
BDA-01	<i>Lannea acida</i> A.Rich.	D <sup>a</sup>	3 (10)	0.26 $\pm$ 0.01	91.9 $\pm$ 17.1	15.6 $\pm$ 2.4	52.2 $\pm$ 7.6	85.8 $\pm$ 15.6	1.35 $\pm$ 0.16	0.084 $\pm$ 0.008
BDA-01	<i>Terminalia laxiflora</i> Engl.	D <sup>a</sup>	3 (10)	0.46 $\pm$ 0.04	157.9 $\pm$ 18.6	24.6 $\pm$ 4.8	81.1 $\pm$ 10.3	114.5 $\pm$ 7.8	1.99 $\pm$ 0.07	0.18 $\pm$ 0.021
BDA-01	<i>Vitellaria paradoxa</i> C.F. Gaertn.	SD <sup>a</sup>	3 (12)	0.3	121.3 $\pm$ 5.5	13.3 $\pm$ 1.9	51 $\pm$ 13	80.3 $\pm$ 21.9	1.65 $\pm$ 0.33	0.106 $\pm$ 0.013
BDA-02	<i>Cochlospermum planchoni</i> Hook.f. ex Planch.	D <sup>f</sup>	3 (10)	0.29 $\pm$ 0.02	98.8 $\pm$ 5.4	20.3 $\pm$ 0.7	64 $\pm$ 7.3	98.5 $\pm$ 19.8	1.42 $\pm$ 0.08	0.097 $\pm$ 0.005
BDA-02	<i>Terminalia laxiflora</i> Engl.	D <sup>a</sup>	3 (9)	0.4 $\pm$ 0.05	184.2 $\pm$ 13.4	21 $\pm$ 2	76 $\pm$ 2.6	124 $\pm$ 8.8	2.38 $\pm$ 0.23	0.163 $\pm$ 0.025
BDA-02	<i>Terminalia macroptera</i> Guill. & Perr.	D <sup>a</sup>	3 (9)	0.39 $\pm$ 0.04	166.8 $\pm$ 15.9	20.8 $\pm$ 0.9	64.3 $\pm$ 2.2	91.3 $\pm$ 6.2	2.13 $\pm$ 0.32	0.15 $\pm$ 0.018
MLE-01	<i>Combretum ghasalense</i> Engl. & Diels.	BD <sup>d</sup>	3 (9)		122 $\pm$ 21.2	13.2 $\pm$ 0.5	45.7 $\pm$ 4.2	74.9 $\pm$ 9.4	1.72 $\pm$ 0.31	0.108 $\pm$ 0.021
MLE-01	<i>Lannea acida</i> A.Rich.	D <sup>a</sup>	3 (9)		104.7 $\pm$ 10.2	11.9 $\pm$ 1.4	40.9 $\pm$ 3.8	70.1 $\pm$ 5.6	1.43 $\pm$ 0.02	0.129 $\pm$ 0.015
MLE-01	<i>Maytenus senegalensis</i> (Lam.) Exell	D <sup>a</sup>	3 (9)		136.8 $\pm$ 19	11.8 $\pm$ 2.3	38.9 $\pm$ 3.8	63.6 $\pm$ 7	1.6 $\pm$ 0.3	0.13 $\pm$ 0.006
MLE-01	<i>Terminalia avicennioides</i> Guill. & Perr.	D <sup>a</sup>	3 (9)		137.5 $\pm$ 9.7	19.2 $\pm$ 0.3	62.7 $\pm$ 2.6	97.5 $\pm$ 3.1	2.06 $\pm$ 0.06	0.128 $\pm$ 0.011
MLE-01	<i>Vitellaria paradoxa</i> C.F. Gaertn.	SD <sup>a</sup>	3 (10)		111 $\pm$ 1.8	8.5 $\pm$ 0.7	38 $\pm$ 5.2	64.2 $\pm$ 10.7	1.46 $\pm$ 0.16	0.087 $\pm$ 0.016
KOG-01	<i>Anogeissus leiocarpus</i> Guill. & Perr.	D <sup>a</sup>	1 (3)	0.23	88.3	10.8	44.4	78.9	1.31	0.218
KOG-01	<i>Chromolaena odorata</i> (L.) R.M.King & H.Rob.	D (most likely)	3 (3)	0.18 $\pm$ 0.02	38.6 $\pm$ 7.9	14.6 $\pm$ 1.6	46.6 $\pm$ 6.9	67.5 $\pm$ 11.3	1.06 $\pm$ 0.09	0.088 $\pm$ 0.003
KOG-01	<i>Daniellia oliveri</i> Hutch. & Dalziel.	D <sup>a</sup>	1 (1)	0.17	94.1	10.1	40.1	64.7	1.82	0.111
KOG-01	<i>Lannea kersingii</i> Engl. & K.Krause	D <sup>c</sup>	1 (1)	0.31	116.7	7.1	32.2	52.2	1.68	0.205
KOG-01	<i>Parinari polyandra</i> (Benth.) Dandy	BD (most likely)	1 (2)	0.25	114.9	10.9	38.5	63.8	2.15	0.13
KOG-01	<i>Pterocarpus erinaceus</i> Lam.	D <sup>a</sup>	1 (3)	0.22	68.5	9.9	37.2	61.8	1.69	0.127

KOG-01	<i>Terminalia glaucescens</i> Planch. Ex Benth.	D <sup>i</sup>	2 (5)	0.3 ± 0.04	119.9 ± 4.7	11.5 ± 4.8	52.2 ± 17.7	86 ± 28.7	2.17 ± 0.02	0.183 ± 0.025
KOG-01	<i>Vitellaria paradoxa</i> C.F. Gaertn.	SD <sup>a</sup>	1 (1)	0.27	132.8	6.1	40.2	66.3	1.97	0.169
BFI-01	<i>Adansonia digitata</i> L.	D <sup>a</sup>	1 (4)	0.26	67.6	8.1	41.1	81.4	1.49	0.171
BFI-01	<i>Anogeissus leiocarpus</i> Guill. & Perr.	D <sup>a</sup>	2 (6)	0.18 ± 0.02	58.2 ± 5.8	6 ± 0.3	34.2 ± 0.9	71.6 ± 12.5	1.4 ± 0.07	0.102 ± 0.015
BFI-01	<i>Holarthra floribunda</i> T. Durand & Schinz	SD <sup>a</sup>	1 (3)	0.19	59.8	6.3	28.9	62.8	1.66	0.122
BFI-02	<i>Anogeissus leiocarpus</i> Guill. & Perr.	D <sup>a</sup> , leaf shed seasonal but seldom completely leafless <sup>b</sup>	2 (5)	0.23	85.1 ± 0.8	11 ± 2.4	44.9 ± 4	68.1 ± 12.5	1.44 ± 0.16	0.148 ± 0.01
BFI-02	<i>Detarium senegalense</i> J.F.Gmel.	D (most likely)	1 (2)	0.36	136.5	9.5	42.9	65.9	2.41	0.139
BFI-02	<i>Lannea acida</i> A.Rich.	D <sup>a</sup>	1 (2)	0.24	96.5	7.6	30.3	49.7	1.75	0.105
BFI-02	<i>Parinari congoensis</i> Engl.	E <sup>i</sup>	1 (3)	0.32	115.3	10.5	39.9	74.9	1.94	0.136
BFI-02	<i>Terminalia glaucescens</i> Planch. Ex Benth.	D <sup>i</sup>	1 (2)	0.33	135.3	11.9	46	54.9	2.42	0.186
BFI-02	<i>Vitex grandifolia</i> Gürke	E <sup>i</sup>	1 (2)	0.4	148	12.9	49.9	89.8	2.21	0.141
BFI-03	<i>Albizia ferruginea</i> Benth.	D <sup>b</sup>	1 (2)	0.16	79.7	5.6	25.3	51.7	2.4	0.09
BFI-03	<i>Antiaris africana</i> Engl.	D <sup>b</sup>	1 (2)	0.4	104.7	10.3	38.2	56.6	2.51	0.105
BFI-03	<i>Ficus saussureana</i> DC.	BD (most likely)	1 (2)	0.36	86.7	10.9	41.8	67.9	1.56	0.095
BFI-03	<i>Holarthra floribunda</i> T. Durand & Schinz	SD <sup>a</sup>	1 (3)	0.26	56.3	11.8	42.3	70.2	1.35	0.11
BFI-03	<i>Khaya antholtheca</i> C.DC.	BD <sup>b</sup>	3 (7)	0.2 ± 0.04	88.4 ± 21.9	6.4 ± 0.5	29 ± 3.2	59.3 ± 12.6	1.84 ± 0.45	0.108 ± 0.01
BFI-04	<i>Blighia sapida</i> Kon.	NCS <sup>b</sup>	1 (1)	0.22	79.7	5.5	26.5	50.1	1.93	0.101
BFI-04	<i>Bosqueia angolensis</i> Ficalho	BD <sup>c</sup>	1 (2)	0.19	63.5	6.9	29.7	41.4	1.27	0.067
BFI-04	<i>Cola caricifolia</i> K.Schum.	E <sup>b</sup>	1 (2)	0.19	65	7.6	35.5	51.1	2.06	0.129
BFI-04	<i>Cola gigantea</i> A.Chev.	D <sup>i</sup>	1 (1)	0.25	116.2	10.6	33.2	49.7	2.28	0.18
BFI-04	<i>Pycnanthus angolensis</i> (Welw.) Exell	E <sup>i</sup>	1 (2)	0.19	64.3	9.5	38.7	63.5	1.79	0.086
BFI-04	<i>Trilepisium madagascariense</i> DC.	E <sup>j</sup>	1 (3)	0.24	69	8.5	31	46.4	1.55	0.149
ASU-01	<i>Corynanthe pachyceras</i> K.Schum.	E <sup>j</sup>	1 (1)	0.15	72.1	6.4	25.1	41.2	1.78	0.064
ASU-01	<i>Hymenostegia afzelii</i> Harns	E <sup>j</sup>	1 (1)	0.16	53.3	5.3	22.1	35.8	1.76	0.083
ASU-01	<i>Nesogordonia papaverifera</i> (A.Chev.) Capuron	NCS <sup>b</sup>	1 (2)	0.15	58	8.1	29.7	48.4	1.66	0.074
ASU-01	<i>Triplochiton scleroxylon</i> K.Schum.	D <sup>b</sup>	2 (6)	0.23 ± 0.02	72.5 ± 0.5	11 ± 1.1	44.9 ± 2.9	76.1 ± 1.6	2.32 ± 0.13	0.127 ± 0.019

<sup>a</sup>de Bie S., Ketter P., Paasse M. & Geerling C. (1998) Woody plant phenology in the West Africa savanna. *Journal of Biogeography* **25**, 883–900.

<sup>b</sup>Hall J.B. & Swaine M.D. (1981) Distribution and ecology of vascular plants in a tropical rain forest. In *Forest vegetation in Ghana. (Geobotany)* (ed Junk W.) p. 398. Springer, The Hague.

<sup>c</sup>Keay R.W.J. (1989) *Trees of Nigeria*. Clarendon Press Oxford, London. p. 476.

<sup>d</sup>Lawson G.W. (1986) *Plant Ecology in West Africa: Systems and Processes*. John Wiley & Sons Inc. p. 376.

<sup>e</sup>Beiter P., Tunbani A.I. & Brittingham M. (2006) Nesting with the wasp *Ropalidia cincta* increases nest success of red-cheeked cordonblue (*Uraeginthus bengalus*) in Ghana. *The Auk* **123**, 1022–1037.

<sup>f</sup>Devineau J.-L. (1999) Seasonal rhythms and phenological plasticity of savanna woody species in a fallow farming system (south-west Burkina Faso). *Journal of Tropical Ecology* **15**, 497–513.

<sup>g</sup>Lieberman D. (1982) Seasonality and phenology in a dry tropical forest in Ghana. *The Journal of Ecology* **70**, 791–806.

<sup>h</sup>Poorter L., Bongers F., Kouame F. Y. N. & Hawthorne W.D. (2004) *Biodiversity of West African forests: An Ecological Atlas of Woody Plant Species*. CABI Publishing, Wallingford. p. 528.

<sup>i</sup>Arbnonnier M. (2004) *Trees, Shrubs and Lianas of West African DryZones*. 576p. CIRAD, MARGRAF & MINHN, Wageningen, The Netherlands.

<sup>j</sup>Swaine M.D. (1996) Rainfall and soil fertility as factors limiting forest species distributions in Ghana. *Journal of Ecology* **84**, 419.

D, deciduous; SD, semi-deciduous; E, evergreen; NCS, not clearly seasonal; BD, briefly deciduous.

**APPENDIX B: A-C<sub>i</sub> CURVE FITTING ROUTINE FOR USE WITH 'R'**

```

## This script is a method for fitting a photosynthesis model to response curves of the dependency of assimilation rates over
## CO2 concentrations at the mesophyll.
## The method considers discontinuous nonlinear functions and solves for parameters by minimization of least-squares
## differences between the data and the model.
## The output parameters ( $V_{\text{cmax}}$ ,  $J_{\text{max}}$  (assuming saturating light), TPU, and  $R_d$ ) are computed for temperatures measured
## during the response curve.
## The error term takes into account the number of observations
## Photo = Net photosynthetic carbon assimilation      ( $\mu\text{mol CO}_2 \text{ m}^{-2} \text{ s}^{-1}$ )           Dependent Variable
## Ci = [CO2] inside the leaf                        ( $\mu\text{mol mol}^{-1}$ ) (same as ppm or  $\mu\text{bar}$ )       Independent Variable
##  $V_{\text{cmax}}$  = maximum carboxylation capacity          ( $\mu\text{mol CO}_2 \text{ m}^{-2} \text{ s}^{-1}$ )           Parameter
##  $J_{\text{max}}$  = electron transport rate                 ( $\mu\text{mol CO}_2 \text{ m}^{-2} \text{ s}^{-1}$ )           Parameter
## TPU = triose phosphate utilization                 ( $\mu\text{mol CO}_2 \text{ m}^{-2} \text{ s}^{-1}$ )           Parameter
##  $R_d$  = respiration under light                     ( $\mu\text{mol CO}_2 \text{ m}^{-2} \text{ s}^{-1}$ )           Parameter
## Tleaf = leaf temperature                           ( $^{\circ}\text{C}$ )                          Independent Variable
## Start from a "clean" R environment
      rm(list=ls(all=TRUE))
      detach()
## Load relevant libraries
      library(stats)
## Import data from a text file, skipping 12 initial information lines from a Licor 6400 standard output file. This value might
## change according to individual machine's setup.
      response.curve <- read.table(filename <- choose.files(), skip = 12, header = TRUE)
      attach(response.curve)
# the following prints the names of the variables from the data set, useful to check if file was loaded correctly
      names(response.curve)
## Photosynthesis model based on:
## Farquhar G.D., von Caemmerer S. & Berry J.A. (1980) A biochemical model of photosynthetic CO2 assimilation in leaves
## of C3 species. Planta 149, 78–90
## Sharkey T.D., Bernacchi C.J., Farquhar G.D. & Singsaas E.L. (2007) Fitting photosynthetic carbon dioxide response curves
## for C3 leaves. Plant, Cell & Environment 30, 1035–1040
# Model Constants
      O2          <- 21          # Estimated Oxygen concentration at mesophyll - (kPa)
      Kc          <- 40.49       # Michaelis-Menten constant for CO2 (Pa) - von Caemmerer et al. (1994)
      delta_Kc    <- 59356       # activation energy (kJ mol-1) - Badger & Collatz (1977)
# Kc adjusted to actual leaf temperature - (Pa)
      Kc_Tleaf    <- Kc * exp((Tleaf+273.15-298.15)*delta_Kc/(298.15*8.314*(Tleaf+273.15)))
      Ko          <- 24.8        # Michaelis-Menten constant for CO2 (kPa)- von Caemmerer et al. (1994)
      delta_Ko    <- 35948       # activation energy (kJ mol-1) - Badger & Collatz (1977)
# Ko adjusted to actual leaf temperature - (kPa)
      Ko_Tleaf    <- Ko * exp((Tleaf+273.15-298.15)*delta_Ko/(298.15*8.314*(Tleaf+273.15)))
      gstar       <- 3.69        # CO2 compensation point (Pa)- von Caemmerer et al. (1994)
      delta_gstar <- 29000       # activation energy (kJ mol-1) - Jordan & Ogren (1984)
# gstar adjusted to actual leaf temperature - (Pa)
      gstar_Tleaf <- gstar * exp((Tleaf+273.15-298.15)*delta_gstar/(298.15*8.314*(Tleaf+273.15)))
      Km          <- Kc_Tleaf*(1+O2/Ko_Tleaf)
# converts Ci from ppm to Pa
      C <- Ci * Press * 0.001
## Function that contains the model equations and the variables
      ffitt <- function(x){
          Vcmax    <- x[1]      # variable 1
          Jmax     <- x[2]      # variable 2
          TPU      <- x[3]      # variable 3
          Rd       <- x[4]      # variable 4
# electron transport rate fitted to high C values
          aj <- ifelse (C >= 45, Jmax * (C - gstar_Tleaf) / (4*C + 8 * gstar_Tleaf)-Rd, 999)
# ignore intermediary C values (region of co-limitation)
          aa <- ifelse ((C > 30 & C < 45), Photo, 999)

```

```

# carboxylation rate fitted to low C values
av <- ifelse (C <= 30, Vcmax * (C - gstar_Tleaf) / (Km + C) - Rd, 999)
# triose phosphate utilization fitted to the last point of the curve
atpu <- ifelse (C == max(C), 3 * TPU - Rd, Photo)
a <- pmin(av, aj, aa)
adiff <- sum((Photo - a)^2) # least-square minimization
bdiff <- sum((Photo - atpu)^2)
diffsum <- adiff + bdiff # object to be minimized
}
## curve fitting procedure, using the "optim" command. It will vary the variables to get the smallest "diffsum" possible
## initial values (first guess) for the starting point of "optim"
start.values1 <- c(100, 130, 10, 3)
first <- optim(start.values1, ffitt, control = list (maxit = 9000), method = "BFGS")
## calculating the error for the curve fitting
fit.error <- first$value[1] / (length(Photo) - sum(C > 30 & C < 45))
## creates a sequence of CO2 values for the figures
Cseq <- seq(0, 200, 0.5)
# creates values of av based on estimated parameters (Vcmax and Rd)
av1 <- first$par[1] * (Cseq - mean(gstar_Tleaf)) / (mean(Km) + Cseq) - first$par[4]
# creates values of aj based on estimated parameters (Jmax and Rd)
aj1 <- first$par[2] * (Cseq - mean(gstar_Tleaf)) / (4 * Cseq + 8 * mean(gstar_Tleaf)) - first$par[4]
# creates values of atpu based on estimated parameters (TPU and Rd)
atpu1 <- first$par[3] * 3 - first$par[4] + (Cseq / 10^10)
## creating a figure showing the relationship between Photo and [CO2] at the mesophyll
plot (C, Photo, col = "blue", pch = 19, xlim = c(0, 200), ylim = c(-5, 60), ylab = "A (μmol CO2 m-2 s-1)", xlab = "[CO2] at mesophyll-Ci (Pa)")
title(main = c(filename), cex.main = 0.8)
lines (Cseq, av1, col = "red", lwd = "2")
lines (Cseq, aj1, col = "orange", lwd = "2")
lines (Cseq, atpu1, col = "purple", lwd = "2")
text (50, 60, "Vcmax =", pos = 2, col = "red"); text (45, 60, round(first$par[1], digits = 1), pos = 4, col = "red")
text (50, 55, "Jmax =", pos = 2, col = "orange"); text (45, 55, round(first$par[2], digits = 1), pos = 4, col = "orange")
text (50, 50, "TPU =", pos = 2, col = "purple"); text (45, 50, round(first$par[3], digits = 1), pos = 4, col = "purple")
text (160, 0, "Rd =", pos = 2); text (170, 0, round(first$par[4], digits = 2), pos = 4)
text (160, -5, "error =", pos = 2); text (170, -5, round(fit.error, digits = 2), pos = 4)
## end

```

## APPENDIX C

**Table A2.** Regression coefficients of the relationships between leaf photosynthetic capacity ( $V_{\text{cmax-A}}$  and  $J_{\text{max-A}}$ ) and leaf traits (nitrogen content,  $N_A$ ; phosphorus content,  $P_A$ ; and leaf mass to area ratio,  $M_A$ ), presented on area basis. Coefficients are not shown when  $p > 0.05$ . Data was  $\log_{10}$  transformed before analyses

Model	All data	OSS	OSW	SW	SDF
$V_{\text{cmax-A}} = a + bN_A$	$a = 1.57, b = 0.55,$ $r^2 = 0.20$	$a = 1.62, b = 0.55,$ $r^2 = 0.61$	$a = 1.59, b = 0.69,$ $r^2 = 0.27$	$a = 1.52, b = 0.38,$ $r^2 = 0.14$	ns
$V_{\text{cmax-A}} = a + bP_A$	$a = 2.08, b = 0.41,$ $r^2 = 0.12$	$a = 2.17, b = 0.43,$ $r^2 = 0.35$	$a = 2.20, b = 0.49,$ $r^2 = 0.19$	$a = 1.95, b = 0.40,$ $r^2 = 0.18$	ns
$V_{\text{cmax-A}} = a + bM_A$	$a = 0.84, b = 0.43,$ $r^2 = 0.21$	$a = 1.07, b = 0.36,$ $r^2 = 0.37$	$a = 0.98, b = 0.36,$ $r^2 = 0.09$	$a = 1.16, b = 0.23,$ $r^2 = 0.11$	ns
$V_{\text{cmax-A}} = a + bN_A + cP_A$	$a = 1.76, b = 0.45,$ $c = 0.18, r^2 = 0.21$	ns	ns	ns	ns
$V_{\text{cmax-A}} = a + bN_A + cM_A$	$a = 1.04, b = 0.34,$ $c = 0.29, r^2 = 0.26$	ns	$a = 2.42, b = 1.08,$ $c = -0.44, r^2 = 0.32$	ns	ns
$V_{\text{cmax-A}} = a + bP_A + cM_A$	$a = 1.15, b = 0.17,$ $c = 0.36, r^2 = 0.23$	$a = 1.53, b = 0.23,$ $c = 0.23, r^2 = 0.42$	ns	ns	ns
$V_{\text{cmax-A}} = a + bN_A + cP_A + dM_A$	ns	ns	$a = 3.13, b = 0.95,$ $c = 0.34, d = -0.62,$ $r^2 = 0.36$	ns	ns
$J_{\text{max-A}} = c + dN_A$	$c = 1.76, d = 0.48,$ $r^2 = 0.20$	$c = 1.79, d = 0.48,$ $r^2 = 0.49$	$c = 1.77, d = 0.70,$ $r^2 = 0.10$	$c = 1.77, d = 0.29,$ $r^2 = 0.09$	$c = 1.66, d = 0.36,$ $r^2 = 0.11$
$J_{\text{max-A}} = c + dP_A$	$c = 2.23, d = 0.36,$ $r^2 = 0.13$	$c = 2.23, d = 0.32,$ $r^2 = 0.20$	$c = 2.35, d = 0.45,$ $r^2 = 0.19$	$c = 2.14, d = 0.35,$ $r^2 = 0.11$	ns
$J_{\text{max-A}} = c + dM_A$	$c = 1.16, d = 0.37,$ $r^2 = 0.21$	$c = 1.34, d = 0.30,$ $r^2 = 0.27$	$c = 1.13, d = 0.38,$ $r^2 = 0.11$	ns	ns
$J_{\text{max-A}} = d + eN_A + fP_A$	$d = 1.95, e = 0.38,$ $f = 0.17, r^2 = 0.22$	ns	ns	ns	ns
$J_{\text{max-A}} = d + eN_A + fM_A$	$d = 1.34, e = 0.30,$ $f = 0.24, r^2 = 0.26$	ns	$d = 2.57, e = 1.07,$ $f = -0.42, r^2 = 0.39$	ns	ns
$J_{\text{max-A}} = d + eP_A + fM_A$	$d = 1.46, e = 0.17,$ $f = 0.29, r^2 = 0.23$	ns	ns	ns	ns
$J_{\text{max-A}} = e + fN_A + gP_A + hM_A$	ns	ns	$e = 3.04, f = 0.99,$ $g = 0.23, h = -0.54,$ $r^2 = 0.41$	$e = 2.78, f = 0.53,$ $g = 0.42, h = -0.36,$ $r^2 = 0.24$	ns

ns, non-significant; OSS, open Sudan savanna; OSW, open savanna woodland; SW, savanna woodland; DF, semi-deciduous dry forest.